TESTING AGGREGATE BACKFILL FOR CORROSION POTENTIAL

By

Zachary A. Brady

Submitted to the graduate degree program in Civil, Environmental, and Architectural Engineering and the Graduate Faculty of the University of Kansas in partial fulfillment of the requirements for the degree of Master of Science.

_____

Chairperson Dr. Robert L. Parsons, Ph.D., P.E.

_____

Dr. Jie Han, Ph.D., P.E., F.ASCE

_____

Dr. Masoud Darabi, Ph.D.

Date Defended: April 22nd, 2016

The Thesis Committee for Zachary A. Brady

certifies that this is the approved version of the following thesis:

TESTING AGGREGATE BACKFILL FOR CORROSION POTENTIAL

_____

Chairperson Dr. Robert L. Parsons, Ph.D., P.E.

Date approved: April 22nd, 2016

Acknowledgements

I thank my parents, Jon and Joanna Brady, for supporting me in my valuable college career, my sister, Erin Brady, for tolerating me and my late nights in the office, and Bill and Marnie Clawson for encouraging me to pursue civil engineering in the first place.

Thank you to my advisors, Robert L. Parsons, Ph.D., P.E.; Jie Han, Ph.D., P.E., F.ASCE; and Masoud Darabi, Ph.D. for their expertise and guidance throughout this study.

I also thank the Kansas Department of Transportation (KDOT) and the Kansas Transportation Research And New-Developments Program (K-TRAN) for providing the financial support for the research described in this thesis; Dr. Stacey Kulesza and Mr. Michael Snapp of Kansas State University for providing field data and technical support for this research; Mr. Jim Brennan of KDOT, Mr. Bill Beggs of Martin Marietta, and Dr. Edward Peltier and Mr. Michael Panethiere, both of the University of Kansas, for providing technical support for this research; Mr. Stephen Lorson of Professional Engineering Consultants (PEC) for providing Pittsburg material field data; Mr. Matthew Maksimowicz, Mr. Kent Dye, and Mr. David Woody of the University of Kansas for their assistance in fabricating the test boxes, and Mr. Madan Neupane and Mr. Jim Jacobe for their assistance with material collection.

Abstract

The Kansas Department of Transportation (KDOT) has designed and constructed numerous mechanically stabilized earth (MSE) walls to support new and expanded highway projects throughout Kansas. MSE walls often contain galvanized steel strips as mechanical reinforcement within layers of specified backfill material. Inclusion of these strips creates a stronger composite material connected to a visually appealing wall facing, however galvanized steel reinforcement is potentially vulnerable to corrosion.

Corrosivity of MSE backfill is typically characterized using electrical resistivity among other properties. KDOT currently uses the American Association of State Highway and Transportation Officials (AASHTO) standard T 288 to calculate the resistivity of MSE backfill. There is concern that this method may not reflect field conditions well, and thus may mischaracterize the corrosivity of backfill. AASHTO T 288 tests were conducted as a part of this research, and the condition of these samples during testing was not consistent with expected field conditions.

A new procedure has been proposed to ASTM that appears to more accurately simulate field conditions behind MSE walls. This ASTM C XXX-XX (the New ASTM) has been extensively tested and compared with AASHTO T 288 in this experimental study. The New ASTM simulated expected field conditions more accurately than the AASHTO test. Results also appear to indicate the need for a larger resistivity box to accurately characterize the corrosivity of larger aggregates. Preliminary recommendations for box geometry are 8:1 minimum electrode spacing to maximum particle size and 3:1 minimum height to maximum particle size. It was also observed that increasing the number of soak/drain cycles of the material resulted in a substantial increase in resistivity values that plateaued at a higher value than observed for both the AASHTO and proposed ASTM methods.

Table of Contents

List of Figures

List of Tables

Chapter 1: Introduction

Mechanically Stabilized Earth (MSE) retaining walls have been used for several decades to support bridge structures, hold excavated slopes in place, and to support new highway and highway widening projects. As MSE wall design developed in the early 1970s, steel was the most popular material used to reinforce soil masses due to its low cost, high strength, and high availability. However, when steel is buried underground it reverts back to a natural ore-like state. The refined iron used to make steel will give up its mechanical bond with carbon and other elements in favor of a lower-energy atomic bond with oxygen, which will convert the iron into an iron oxide state. This oxidation reaction is the process of rusting, or corrosion.

1.1: Galvanization Corrosion Process

The consequences of corrosion of metal reinforcement in MSE walls were quickly realized and mitigation efforts were implemented. Almost all steel used to reinforce earth masses is now galvanized, or coated with a layer of pure zinc. The presence of zinc protects the steel in three stages: the zinc patina barrier protection, the barrier of protection composed of steel-zinc alloy layers, and cathodic protection. As soon as the galvanization process is complete, the pure zinc layer will begin to react with water in the air. After 6-12 months of wet-dry cycles on the pure zinc surface, electrons will have relocated sufficiently to form a much harder patina composed of zinc carbonate, which is insoluble in water and corrodes at $1/30^{th}$ the rate of bare steel in the same environment. As this zinc patina breaks down, the underlying steel-zinc layers will begin to corrode until the bare steel is exposed. At this point, cathodic protection takes over, during which the remaining galvanization layers and the bare steel are all in contact with the soil environment. This forms a bimetallic couple, or a galvanic battery cell, in which electrons are transferred from the anode (galvanization layers) to the cathode (bare steel) due to the higher electron

affinity of iron. In this way, even though the bare steel is exposed, as long as there is zinc nearby, it will not oxidize or corrode. Zinc is also the preferred coating due to its natural occurrence in soil, which eliminates the potential for contamination. For a more theoretical review of galvanic corrosion, see Oldfield (1988).

1.2: Effect of Resistivity on Corrosion Potential

The bulk electrical resistivity of a material is influenced by both its bulk density and moisture content (Hazreek, 2015), which indicates that electrochemical corrosion rates of metal reinforcement behind MSE walls are also influenced by the bulk density and moisture content of the backfill. Escalante (1988) conducted galvanic corrosion current measurements on underground bimetallic couples over a four-year period and found that in well aerated soils, resistivity greatly controls the corrosive galvanic current. Thus, the generally accepted inverse proportionality of soil electrical resistivity to its corrosion potential was determined valid for aggregate backfills.

1.3: Archie's Law and Electron Transport through Porous Media

Gus Archie (1942) developed an empirical equation set to estimate the saturation of porous media that indicated tortuosity, porosity, resistivity of the pore fluid, cementation, and saturation all affect the bulk resistivity of porous media. Bulk resistivity is what is calculated from the measured bulk resistance using a two-electrode soil box method.

Tortuosity describes the arrangement and crookedness of interconnected pores between soil particles. Regarding electron movement and assuming electrons flow mostly through the pore fluid of saturated porous media, the higher the tortuosity of a saturated aggregate sample, the longer the typical electron flow path will be. Resistivity of the pore fluid (almost always water in MSE backfill) is affected by both the number and types of ions dissolved in the fluid, especially from salt on the roadways that is

pushed to the side of the roadway and into the top of the MSE wall. Cementation describes the deposition of precipitates from the pore fluid onto the boundaries of the pore spaces. This directly influences both the porosity and tortuosity of the aggregate, and thus affects its resistivity.

Saturation of pore spaces affects resistivity of MSE backfill by influencing the electron flow path. If the backfill material pores are 100 % filled with air and if the air is assumed to be much more electrically resistive than the aggregate, then electrons will tend to travel through aggregate particles and their contact points. Once saturation rises above 0 %, pores are partially filled with fluid, and due to the adhesion of the fluid to the aggregate particles, pore fluid coats aggregate particles. As soon as this coating forms, ions from the particle and the air are dissolved into the pore fluid, which decreases the resistance to electron flow in the pore fluid so that electron transport occurs mostly around aggregate particles and through their contact points. This adjustment to the electron flow path affects aggregate resistivity. In fully saturated aggregate backfill, the majority of the electron flow will often occur via interconnected pore spaces because the electrical resistivity of the pore fluid with dissolved ions tends to be much lower than that of the aggregate particles themselves.

1.4: MSE Wall Galvanized Steel Reinforcement Design: Electrical Resistivity

The corrosion protection offered by galvanization prompted the development of sacrificial galvanization thickness requirements for metal reinforcement based on the corrosivity of the soil used for MSE backfill. The corrosivity of MSE backfill is typically characterized by its electrical resistivity; pH; and organic, sulfates, and chlorides contents. This research focuses on the determination of a material's electrical resistivity, which can be calculated from measurements of apparent resistance in the field or the laboratory. AASHTO has developed a standard method to measure the apparent electrical resistance and then calculate the resistivity of soil using a two-electrode soil box (AASHTO T 288). The soil box is constructed from chemically fused polycarbonate sheets and has two stainless steel electrode plates

connected to the long, opposite, interior sides. These plates are connected to exterior stainless steel posts designed to connect to a resistivity meter. Electric current is passed from one electrode through the soil sample to the other electrode, and the resulting voltage difference between the two electrodes is measured. Using Ohm's law, this voltage difference is converted into a measure of resistance in ohms. The resistance is then multiplied by a factor that is a function of box geometry to calculate the electrical resistivity of the material inside the box.

1.5: Representative Volume Element: AASHTO Two-Electrode Soil Box

For any laboratory results applied to the field, there must be confidence that laboratory test conditions allow results to be accurately extrapolated to the field scale. This confidence may be obtained by determining the representative volume element (RVE) of the field material considering the test method. The RVE of a material typically considers its maximum particle size, uniformity of the particle size distribution, and field compaction level among other material properties.

The two-electrode soil box was developed to be an RVE of the soil it was testing. That is, the laboratory results in the two-electrode soil box should be able to be used to represent the entire backfill material of interest. Similarly, the AASHTO T 288 box should be an RVE from which the results may be used to represent the MSE backfill as a whole in the field. As backfills have increased in particle size, concerns have arisen that the AASHTO box no longer provides the required RVE for aggregates.

In addition to maximum particle size, uniformity, and other material properties, Pellinen et al. (2015) determined that the RVE of a comparable composite material to MSE wall backfill, asphalt pavement, depends upon the electrical frequency or resolution of the electromagnetic measurement method. Thus, everything else being constant, two resistivity meters using two different frequencies to measure resistance in the same two-electrode soil box with the same material inside may give dissimilar results.

1.6: AASHTO T 288 Electrical Resistivity Test Applicability to MSE Wall Backfill

In recent years, the backfill material used in MSE walls constructed for KDOT has shifted from sands to crushed limestone aggregates. Since corrosion is still of significant concern, resistivity testing is still conducted. However, there has been concern that the AASHTO T 288 test does not accurately provide the true resistivity of the aggregate backfill for several reasons. These reasons include the small size of the AASHTO resistivity box compared with typical aggregate particle sizes. Size is an issue because the box may be too small to allow repeatable laboratory determinations of electrical resistivity for samples containing larger aggregate particle sizes. Also, since the original AASHTO T 288 standard was developed for use with finer-grained soils, there is concern that the procedure used to determine the electrical resistivity of the MSE aggregate backfill does not accurately represent field conditions of the aggregate, and thus does not give results useful for the design of MSE wall metal reinforcement. This research explores the applicability of the AASHTO T 288 standard to aggregate backfill, the effectiveness of the New ASTM method to calculate the electrical resistivities of aggregates that better represents MSE wall backfill field conditions, and the approximate size of box required to accurately and repeatably calculate aggregate electrical resistivity using the New ASTM method.

The format of the remainder of this thesis is as follows: Chapter 2 contains a review of the relevant literature; Chapter 3 contains a description of the scope of work of this study, procedures followed and equipment used; Chapter 4 contains the results of testing and subsequent analysis; and Chapter 5 contains the conclusions and recommendations developed from this research.

Chapter 2: Literature Review

Corrosion of metal reinforcement in MSE walls has been of concern since the earth reinforcement technique was brought to the United States in the 1970s. As larger limestone aggregates have become more widely used as backfill for MSE walls in Kansas, it is now more crucial to characterize their corrosive properties. One of the most important properties of MSE wall backfill is electrical resistivity, which is currently calculated using AASHTO T 288. There is concern that AASHTO T 288 may not yield resistivity results that are accurate or repeatable for larger aggregates since the standard was developed for use with finer-grained soils.

Studies have been published regarding characterizing the resistivity of larger aggregates in the laboratory. A summary of selected research is presented in this chapter.

2.1: MSE Wall Overview

The earth reinforcement technique is used to build higher and stronger embankments and more stable transportation structures and was developed in pre-1970 France before it quickly spread worldwide. Layers of metal reinforcement strips or meshes are included within layers of backfill material during construction; the resulting mass acts as a much stronger composite material. The first, and still very common, reinforcement material used for these structures was galvanized steel, and many MSE walls with steel reinforcement have been built in Kansas.

2.2: Galvanized Steel Anatomy

According to the American Galvanizers Association (AGS), the galvanization process results in multiple layers of different steel-zinc alloys covered by a layer of pure zinc and underlain by the bare steel surface. These alloy layers adhere strongly to the steel and protect it from corrosion for up to 75 years, depending upon environmental conditions. They consist of hard, abrasion-resistant material overlain by

a soft, ductile layer of pure zinc, which provides impact resistance in addition to the abrasion resistance provided by the alloy layers. Since the steel is fully immersed in molten zinc, these layers provide 99 to 127 µm of corrosion barrier protection uniformly on every exposed surface (AGA, 2012).

2.3: Galvanized Steel Reinforcement Corrosion

As the freshly galvanized steel article is exposed to the air, oxidation of the top pure zinc layer begins, forming oxides of zinc. After the steel article is placed in the ground and is subject to enough wetting and drying cycles, a layer of strong, adhesive zinc carbonate (the dull grey zinc patina) forms. The new zinc carbonate layer is insoluble in water, which protects the remainder of the zinc layer from corrosion and reduces the corrosion rate of the newly patinated galvanized steel article to $1/30^{th}$ that of bare steel in the same conditions. Depending on environmental conditions and the frequency of wetting and drying cycles, this patina takes anywhere from six months to a year to fully develop (AGA, 2012).

The zinc patina is the first of two stages in barrier protection to prevent corrosion of structural steel. The second stage in barrier protection is composed of the underlying steel-zinc alloy layers. As long as the bare steel remains unexposed to the outside environment, the abrasion resistant alloy layers provide the steel with a hard, adhesive layer of protection from the corrosive environment.

When the zinc patina and alloy layers are breached, cathodic protection becomes the primary means of preventing corrosion of the steel. During cathodic protection, the two-stage barrier protection provided by the zinc patina and its underlying alloy layers is compromised due to thinning. As these barriers thin, the steel becomes more and more directly electrically connected to the outside environment, increasing its own corrosion potential. The remaining zinc will act as the anode since zinc is more galvanically active than steel (iron). The steel will act as the cathode, and the soil environment as the electrolyte in this bi-metallic couple electrical circuit. In a bi-metallic couple, the anode is oxidized and the cathode is protected from oxidation. Since steel is forced to be cathodic by the presence of the

zinc, steel is protected from corrosion, or oxidation. This cathodic protection is effective even when the bare steel is exposed to the outside environment—so long as zinc is present within a certain diameter, the exposed steel will not begin to corrode (AGA, 2012).

Galvanization is advantageous over other corrosion protection methods due in large part to the three-stage protection system offered by the zinc with its two stage barrier protection in addition to its cathodic protection. Also, since zinc is naturally occurring in most soils, its oxidation represents no ground/groundwater contamination potential.

The effectiveness and life span of galvanized steel reinforcement behind an MSE wall depends in large part on the corrosion characterization of the material it is embedded in.

2.4: Corrosion Characterization Importance

Failure to accurately characterize the corrosivity of a proposed backfill for an MSE wall can have disastrous consequences, especially for walls designed to last up to 75 years. The Nevada Department of Transportation (NDOT) conducted an investigation into accelerated steel reinforcement corrosion behind several MSE walls in the Las Vegas metropolitan area. NDOT found that the aggregate backfill that was accepted for wall construction in 1985 based on an NDOT standard of electrical resistivity should have been rejected for MSE use due to its chemical aggressiveness, based on tests conducted during the study. The walls in question were reinforced with nongalvanized welded wire fabric (Thornley et al., 2010). A separate investigation conducted by an Ohio consulting firm of another retaining wall reinforced with nongalvanized steel revealed several failed tieback anchors within two years after construction due to accelerated corrosion of the anchor rods (Esser and Dingeldein, 2007).

Other studies of properly galvanized steel reinforced MSE walls showed lower-than-predicted corrosion of both galvanized and nongalvanized MSE wall pullout coupons in Utah (Billings et al., 2011)

and of galvanized reinforcement samples in Kentucky (Beckham, Sun, and Hopkins, 2005). These MSE wall backfills were accepted based on AASHTO standards. The Association of Metallically Stabilized Earth (AMSE) offered a potential explanation for these consistently lower-than-predicted corrosion rates when it stated that the AASHTO specifications may have more than doubled the recommended assumption for galvanization thickness loss per year for use in corrosion models that was presented in the original research data (AMSE, 2006).

2.5: Underground (Soil) Corrosion

Corrosion of underground metal has been studied extensively by several departments of transportation (DOTs), federal agencies, and engineering organizations. Underground electrolytic corrosion studies of metal pipe were published as early as 1895 in Transactions of the American Institute of Electrical Engineers (Low, 1895). Stray current from electric rails was the main concern. Another major published study was the 45-year underground corrosion study of various metals and their coatings conducted by the U.S. Department of Commerce National Bureau of Standards in its Circular 579 (Romanoff, 1957). Romanoff focused on the finer-grained soil electrochemical properties, which offered useful insight for future researchers in determining how grain size distribution, moisture content, temperature, electrical resistivity, and various other soil properties affected corrosion rates.

Corrpro Companies Inc. developed and verified methods to measure the laboratory and field corrosivities of soil based on estimated resistivities for buried pipe applications (Vilda III et al., 2009). Elias of the Federal Highway Administration (FHWA) focused research efforts on applying Romanoff's data for galvanized steel to MSE wall reinforcement corrosion (Elias, 2000).

2.6: MSE Backfill Corrosivity

As MSE walls with galvanized steel reinforcement became popular post-1970, the corrosion research foundation laid by Romanoff and others acted as the basis for estimating MSE metal reinforcement corrosion. However, many researchers found that soil corrosivity characterization techniques for soil could not be effectively applied to aggregates. When subjected to leachate testing, different particle size ranges within a given aggregate exhibited different electrochemical properties (Thapalia et al., 2011).

Castillo et al. proposed a method using an unsieved sample to address the particle-size-driven electrochemical property differences. This test essentially gave the average of the different electrochemical properties of the different particle sizes with one test on the liquid obtained from a leachate test (Castillo et al, 2014). This method did address Thapalia et al.'s findings above, but still may not be representative of actual field conditions. The previous researchers from Lowe in 1895 to Castillo in 2014 had shown that electrical resistivity can effectively represent corrosivity, so the challenge then became how to accurately determine electrical resistivity of larger aggregates.

Edlebeck and Beske (2014) of the Institute of Electrical and Electronics Engineers (IEEE) developed a laboratory procedure to estimate the electrical resistivity of larger aggregates using electrical substation ground covering. This material is similar to MSE coarse aggregate backfill in both particle size and desired electrochemical property determinations. A known mass of unsieved material was first prepared to a specific moisture content and then was compacted into a known volume container (in this case, a 0.4 ft^3 concrete block mold). The resistance of the material was measured using a Wenner 4-probe arrangement modeled from a combination of ASTM G57 and G187 (Edlebeck and Beske, 2014). This procedure controls major electrical resistivity influences such as moisture content and compaction.

2.7: Research Directions for MSE Backfill Corrosion Potential Characterization

Based on the literature, control of density for corrosion characterization of MSE coarse aggregate backfills in accordance with Edlebeck and Beske's methods for electrical substation ground cover should be considered. Underground corrosion studies of metal reinforcement are recommended to consider only galvanized steel reinforcement due to its advantages and popularity compared with other corrosion protection methods. Thapalia et al. recommend that samples for laboratory characterization not be sieved to a certain size due to the potential for different aggregate fractions to have different electrochemical properties. Yzenas Jr. (2014) has proposed a procedure to ASTM International as a New ASTM in which an unsieved aggregate sample is compacted into a two-electrode box, soaked in a specific type of water for 24 hours, drained, and then is tested to estimate electrical resistivity. The procedure of the New ASTM satisfies many of the perceived shortcomings associated with the AASTHO T 288 method.

The following chapters illustrate differences between the New ASTM and the current AASHTO method for electrical resistivity of aggregates and explore the New ASTM's applicability, repeatability, and possible procedural improvements.

Chapter 3: Research Scope

This chapter contains descriptions of the scope of work for this project, the materials used, and the tests performed on them. The standard AASHTO electrical resistivity test and the draft of a new ASTM aggregate resistivity test were both used according to their respective procedures except where noted. In addition to the research conducted at the University of Kansas (KU), Kansas State University (KSU) conducted field electrical resistivity tests on the same materials after their placement as backfill.

3.1: Materials Used

Five backfill samples were collected from four different retaining walls near the ends of their respective construction phases. This eased material collection and provided material as close to field conditions as could be achieved, but also limited material collection to specific times. Sampling collection locations are reported in Table 3.1. All locations were in Kansas.

Table 3.1: Sample Collection Locations

Material	Collection Location
Colored I70/K7	I70/K7 Interchange, SW Ramps from I70 to K7, N of Bonner Springs
Gray I70/K7	I70/K7 Interchange, SW Ramps from I70 to K7, N of Bonner Springs
Pittsburg	Meadowbrook Mall, Pittsburg, NW Wall along Centennial Drive
Ridgeview	N Bridge Abutment on S Ridgeview Rd. crossing K10 W of Lenexa
SLT	N Wall along new 31st St. E of Haskell Intersection, Lawrence (South Lawrence Trafficway)

Sampling details are reported in Table 3.2 on the following page. The I70/K7 wall near Bonner Springs, Kansas provided two visually different aggregate backfills—samples of both were collected. Material was manually collected in large trash cans in accordance with ASTM D75 unless noted otherwise. The sample size for each type of material was approximately 800 pounds (five 20 gal. trash cans, each approximately 2/3 full). Trash can lids were taped shut on the way back from collection to prevent material contamination and loss.

Table 3.1: Sampling Details

Material	Wall Length	Wall Max Height	Wall Type	Collection Source	Collect Date	Max Size	Color
Colored I70/K7	1160 ft. (353 m)	38 ft. (11.5 m)	Geogrid MSE	Stockpile ASTM D75	6/16/14	1" (25 mm)	Multi
Gray I70/K7	1160 ft. (353 m)	38 ft. (11.5 m)	Geogrid MSE	Compacted Backfill	6/23/14	1" (25 mm)	Gray
Pittsburg	380 ft. (116 m)	7 ft. (2.1 m)	Geotextile MSE	Stockpile ASTM D75	7/25/14	1" (25 mm)	White
Ridgeview	230 ft. (70 m)	18 ft. (5.5 m)	Metal SINE-Strip MSE	Compacted Backfill	9/19/14	3" (75 mm)	Orange
SLT	300 ft. (91 m)	16 ft. (4.9 m)	Gravity MSE	Stockpile ASTM D75	2/24/15	¾" (19 mm)	White

A few notes about specific samples are as follows. The gray I70/K7 sample received light rain on top of the trash can lids on the way back from collection. The Pittsburg sample was collected from a stockpile using a front loader. The Ridgeview material visually had more fine particles than the other samples and originated from the Upper Farley ledge in the Sunflower Quarry near De Soto, Kansas.

3.2: Lab Tests

The tests used to characterize the five different materials are listed in Table 3.3 below.

Table 2.3: Material Tests

Standard	Description
AASHTO T27	Sieve Analysis
AASHTO T 288	Soil Electrical Resistivity
the New ASTM	Aggregate Electrical Resistivity

Additional information is provided in the following sections on the tests for which no standard procedure has been established, or for which the procedures for an existing test were modified for the purposes of this research.

3.2.1: AASHTO T 288 Soil Electrical Resistivity Test

AASHTO T 288 required 1500 grams of material smaller than 2 mm in diameter (passing the No. 10 sieve). The material was soaked for at least 12 hours in water that had passed through a battery water deionizer (battery DI water) before being placed into the cleaned AASHTO box using finger pressure for compaction. The AASHTO box was 4.4 cm in inside height, 15.2 cm in inside length, and 9.8 cm in width between the two electrode plates (see Figure 3.1). After compaction and striking off the sample to the level of the top of the box, the filled AASHTO box was then connected to a resistivity meter that met the requirements of AASHTO T 288.

The resistance of the soaked material, its water content, and its wet mass were measured and the density of the material was calculated. The measured material was then removed from the box, mixed with additional battery DI water, and recompacted into the box; the same measurements were taken; this process was repeated until the measured resistance reached a lower limit and then began to increase. Resistivity was then calculated by multiplying this minimum measured resistance by the cross-sectional box area perpendicular to electron flow divided by the average distance between the two electrode plates. This geometric ratio is often called the box factor.

Figure 3.1 shows the AASHTO box dimensions. Figure 3.2 shows the resistance measurement setup.

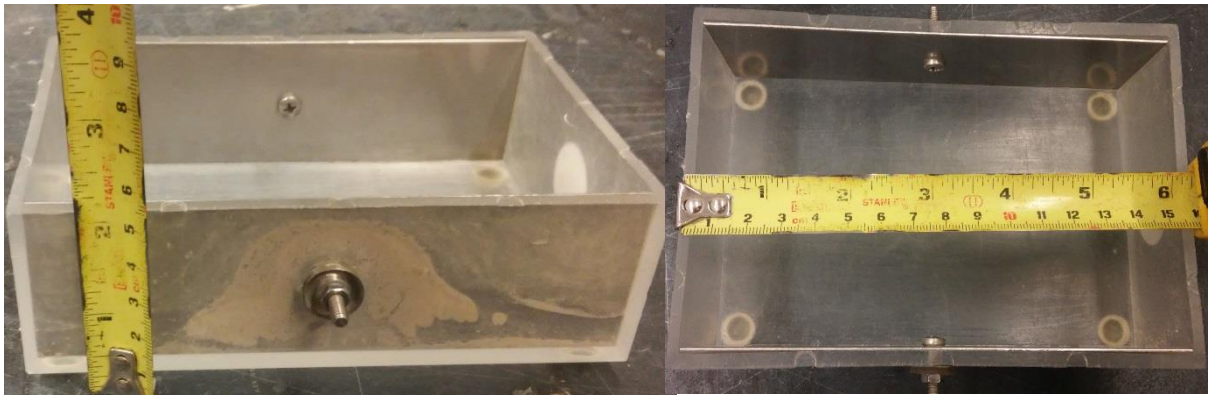

Figure 3.1: AASHTO Electrical Resistivity Box

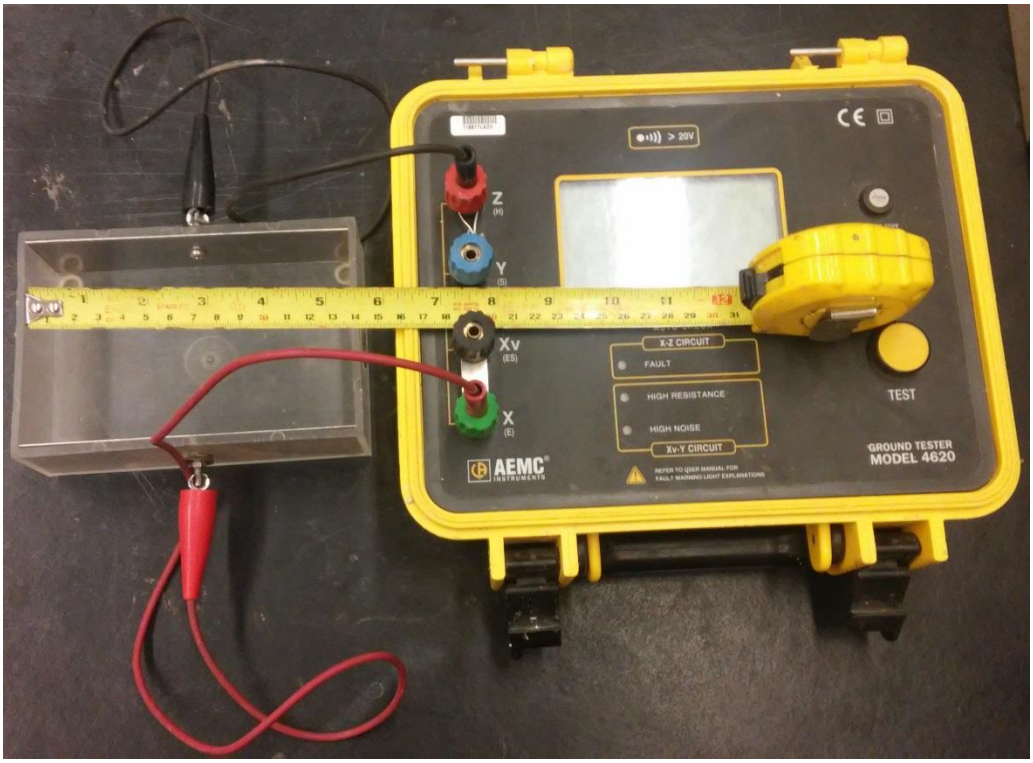

Figure 3.2: AASHTO T 288 Apparatus Setup

3.2.2: The New ASTM Aggregate Electrical Resistivity Test

The primary test used in this research was the most recent draft of a new ASTM aimed at obtaining the electrical resistivity of larger aggregates: ASTM C XXX-XX Coarse Aggregate Resistivity Using the Two-Electrode Soil Box Method. This New ASTM is a new procedure that has been proposed by John J. Yzenas Jr. (2014) for adoption by ASTM. This test procedure differs from AASHTO T 288 in several key ways for aggregate material. A summary of this test is presented in the following paragraph. Subsequent paragraphs describe the manipulation of different test parameters.

3.2.2.1: New ASTM Procedure

The amount of material required to run the New ASTM coarse aggregate resistivity test depended upon the size of the box used. The sample of material was first split to reduce the sample size to approximately match the amount required to fill the particular box; foreign material that should not have been in the sample (leaves, grass, dirt, etc.) was then removed. The split sample was placed into the box in layers no deeper than two (2) inches. Each layer was first wetted with the same battery DI water used in AASHTO T 288 (unless noted otherwise), and was then compacted by alternately lifting and then dropping each side of the box approximately one (1) inch for 25 total drops per layer. After filling and then striking off the top of the material even with the top of the box, the same water type used to wet the aggregate layers was added into the box until full. The sample was then left to soak for 23-25 hours under a covering to prevent contamination. During soaking, similar water was added as needed to maintain 100 % saturation of the sample.

After soaking, the water in the Small, NEMA and Large boxes was allowed to fully drain from the box via gravity, after which point the resistance of the resulting drained material was immediately measured. Full drainage for these boxes was assumed to have occurred when no more pore fluid was observed to drip out of the drain hole.

The ASTM and AASHTO boxes had no drain hole so as to preserve their manufactured form for other testing standards. After soaking, the water in these boxes was vacuum-drained using a wet/dry shop vacuum with 1/8-inch flexible tubing attached to the nozzle. Full drainage was assumed to have occurred when the level of water inside the box reached that of the bottom of the box.

To promote full drainage of the test material, all boxes were tilted toward their respective draining apparatus. This tilt was at first just below the friction angle of the material in the test box, but was reduced to approximately 10° to increase the stability of the sample during draining. The different angles of drainage tilt appeared to have negligible effect on the results.

To calculate the resistivity of the material, the same procedure from AASHTO T 288 was used: measured resistance multiplied by geometric box factor equaled resistivity.

3.2.2.2: New ASTM Testing Parameter Variations

Throughout this research, soaking time, water type used, covering type, the number of soak/drain cycles, and the resistivity meter used during the New ASTM tests were all adjusted to determine their effects on the New ASTM resistivity test results.

Soaking times ranged from 5 hours to 80 hours. Water types used were either the battery DI water or tap water that had passed through a deionizer, an ultraviolet filter, and a reverse osmosis filter (RO UV DI). Rubber-banded plastic wrap was used for covering the boxes during soaking until it was observed that water was being removed from the box via the plastic's capillary action; rigid plastic plating was used for covering the boxes after this behavior was observed.

Several samples were soaked, permitted to drain, and soaked again in an attempt to simulate repeated infiltration cycles in the field. The first soak/drain cycled material (Cycle1) was created using the same material sample as the original New ASTM test. After the initial resistivity measurement, the freshly

drained material was soaked again for a number of hours (typically 24 to follow the New ASTM), drained, and then tested again, giving a result for once-drained material (Cycle1). Cycle2 material was created using the same procedure on the Cycle1 material rather than the original New ASTM test sample, Cycle3 material used Cycle2 material, and so on.

For most tests the AEMC® model 4620 ground resistivity meter was used, which meets the requirements of AASHTO T 288 and costs approximately $2,000. This AEMC® meter has a maximum display limit of 2000 ohm, which is too small for the material used in boxes with smaller geometric box factors, such as the AASHTO box and especially the Miller box (see Figures 3.3 and 3.4 and Table 3.4). This limit corresponds to a sufficiently high resistivity for most boxes so it should not be a problem in practice for pass/fail type testing using the KDOT resistivity standard minimum of 50 ohm-m, but for the purposes of this research and correlation with other material properties, determination of the actual resistivity value was necessary. To address this equipment limitation, the resistivity meter used for KSU's field tests was also used for a few of the Gray I70/K-7 material resistivity tests. This meter, a SuperSting™ R8 IP Earth Resistivity Meter (SSR8), cost over $30,000 but offered a much higher maximum display limit of at least 60,000 ohm, which allowed comparison of ASTM and AASHTO box results with the results for the other boxes.

3.2.2.3: New ASTM Test Boxes

The dimensions of the six different boxes used for New ASTM testing are shown in Table 3.4 below. Pictures of the boxes are shown in Figures 3.1 (AASHTO) and 3.3 through 3.6.

Table 3.3: Electrical Resistivity Box Details

Box Name/ Identification	Height **cm**	Length **cm**	Electrode Separation **cm**	Box Vol. **cm^3**	Box Factor, **cm**
AASHTO	4.4	15.2	9.8	654	6.8
Small	15.0	23.9	7.0	2510	51.2
NEMA	14.5	34.9	24.0	12145	21.1
Large	19.8	45.3	14.9	13320	60.4
Miller	3.3	3.9	19.9	241	0.61
NEMAmod	14.5	34.9	8.8	4428	57.8

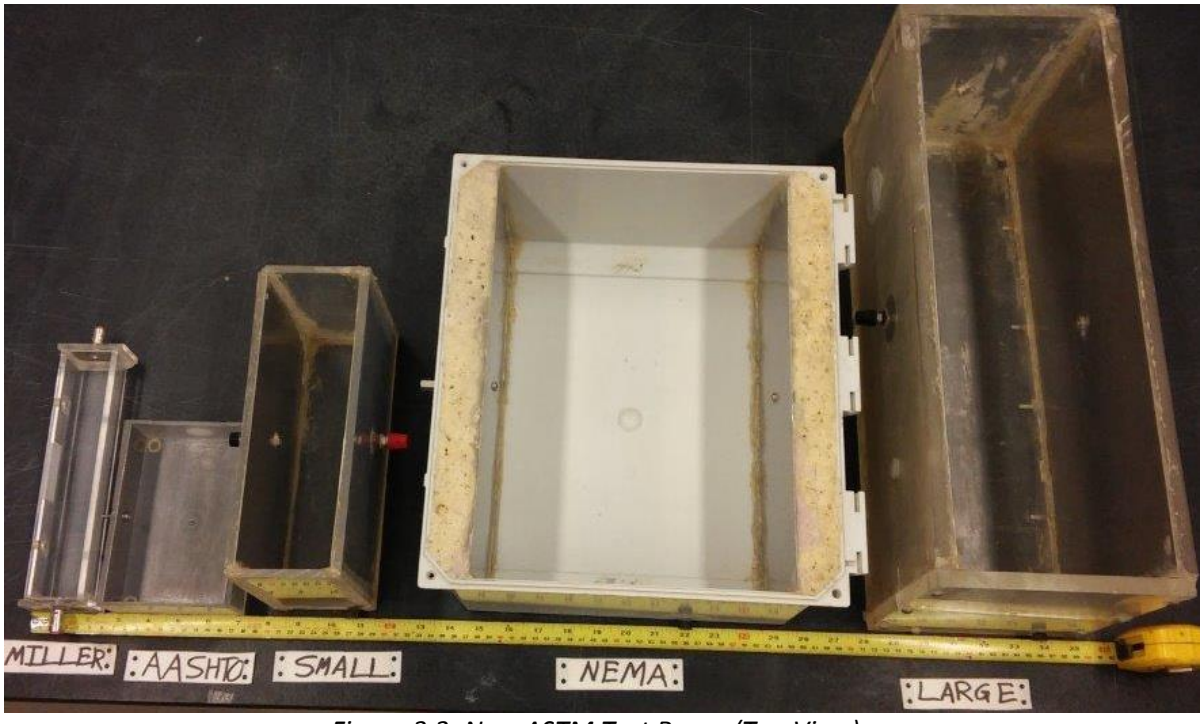

Figure 3.3: New ASTM Test Boxes (Top View)

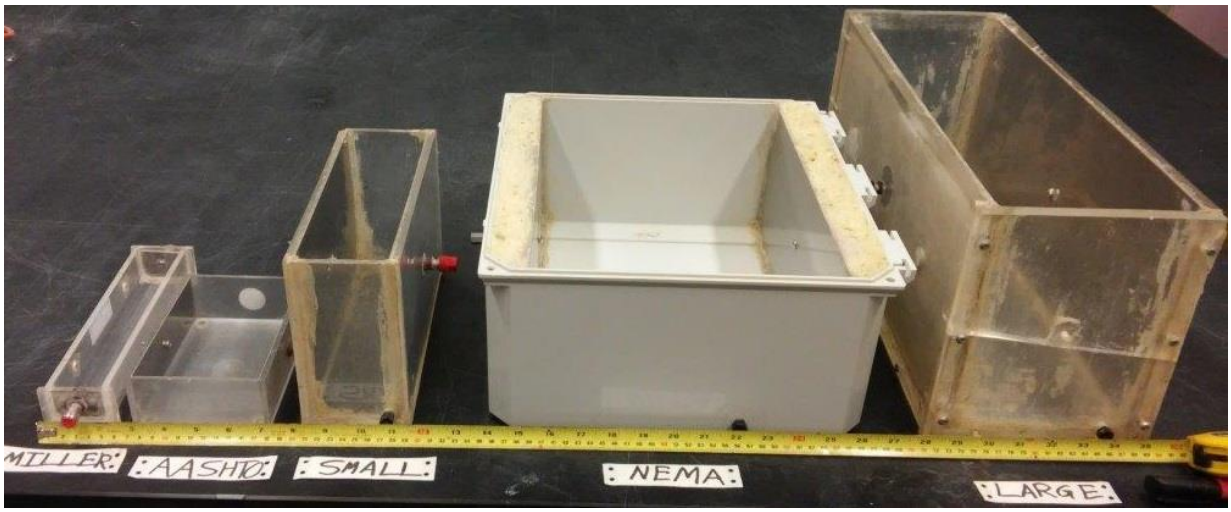

Figure 3.4: New ASTM Test Boxes (Oblique View)

The Small and Large boxes were constructed using polycarbonate sheet connected at right angles edge to edge and sealed with silicone sealant to prevent liquid loss during soaking. The NEMA box started as a commercial, polycarbonate electrical box. Stainless steel electrode plates and the drain plug were installed by KU. The Small, NEMA, and Large boxes each had a drain hole closed by a threaded, plastic drain plug of 9.5 mm outside thread diameter installed to allow water in the box to drain fully. Figure 3.7 shows the NEMA box with its drain plug. The AASHTO and Miller boxes were purchased from manufacturers and were certified to meet the AASHTO and ASTM standards for resistivity, respectively. The NEMAmod box was constructed by modifying the original NEMA box to have a larger box factor by reducing the distance between the electrode plates. This was accomplished by installing 6 inches of insulative foam board cut to the dimensions of the electrode side of the NEMA box between one electrode plate and its side of the NEMA box. The NEMAmod box was used for longer-term cycling tests after all data from the NEMA box was obtained; a higher box factor was necessary to accommodate the AEMC meter maximum reading of only 2000 ohm. Figure 3.5 shows the NEMAmod box dimensions and the modifications mentioned above.

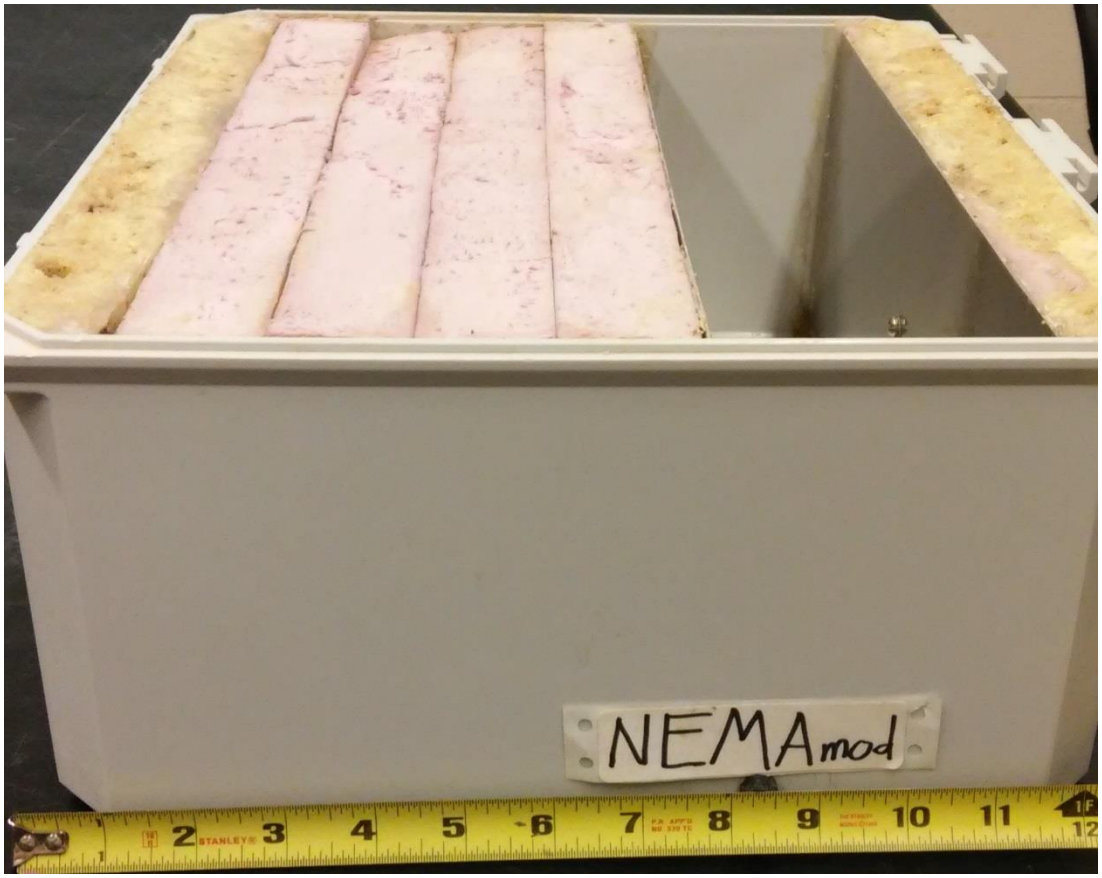

Figure 3.5: NEMAmod Box used for New ASTM Longer-Term Cycling Tests

Figure 3.6: NEMA Box Outside (left) and Inside (right) with Threaded Drain Plug

All boxes were constructed using polycarbonate sheeting thick enough to be rigid during the compaction procedure. The electrode plates in the AASHTO, Small, NEMA, NEMAmod, and Large boxes were all fabricated from stainless steel sheet metal and were cut to exactly match the inside dimensions of the electrode sides of each box. The Miller box electrode plates were installed by the manufacturer and covered approximately 77 % of the curving cross-sectional area of the electrode sides of the box. Gaps behind the electrode plates installed in the Small, NEMA, NEMAmod, and Large boxes were filled with nonconductive, expansive foam where practical and then sealed with silicone to prevent liquid inflow.

The Miller and Large boxes were both initially constructed for 4-probe measurements, but were converted to 2-probe configurations both to follow the New ASTM procedure and to maximize the box factor to maximize the usage of the AEMC® meter 2000-ohm maximum display limit.

Chapter 4: Test Results and Discussion

Figure 4.1 shows the grain size distribution of all five samples tested in this research. Note the Ridgeview and SLT distributions for a diameter near 1 mm. As shown later, these two samples exhibited the lowest resistivity values as measured by the New ASTM test.

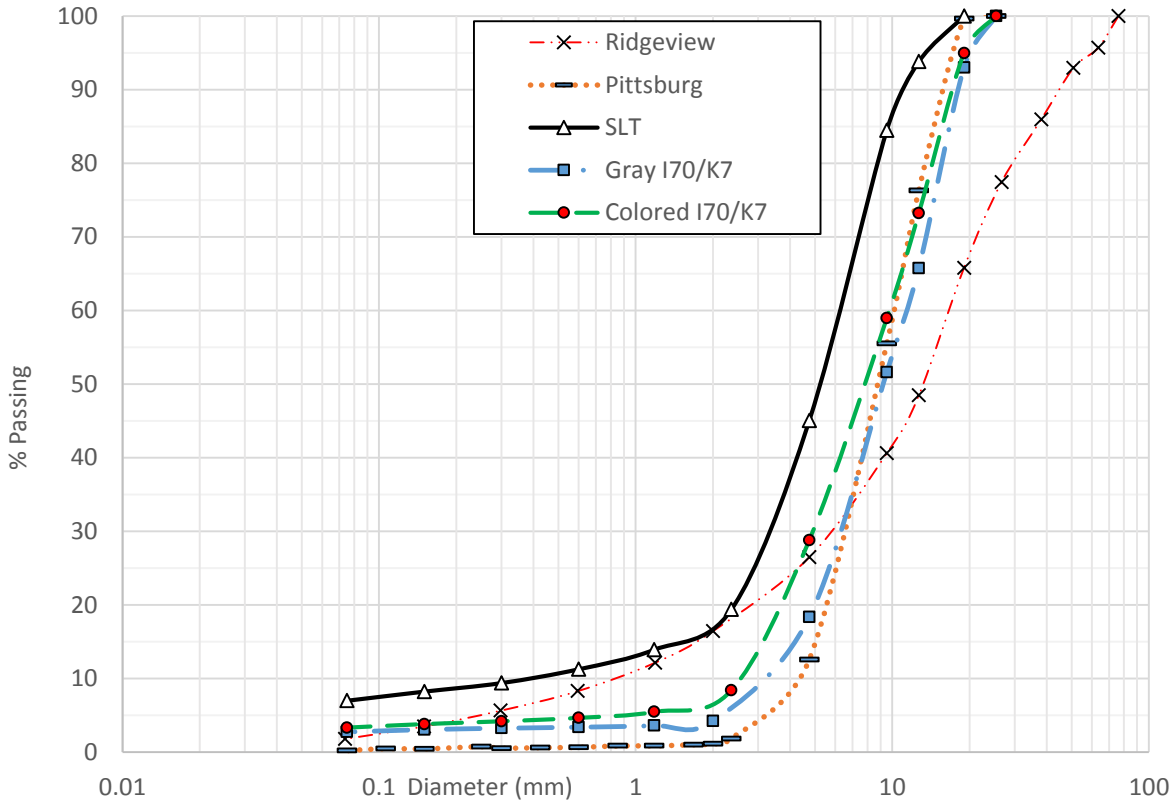

Figure 4.1: Grain Size Distributions of Samples from MSE walls

4.1: AASHTO T 288 Electrical Resistivity

4.1.1: AASHTO T 288 Pittsburg Results

The AASHTO T 288 test was conducted with approximately 1500 g of dry Pittsburg material passing the No. 10 (2 mm) sieve. The 6.48 ohm-m minimum resistivity of occurred at a moisture content of 128 %. The mass of solids compacted into the box in Round R1 was 1223 g; this number was 416 g by Round R11, at which the minimum resistance was measured. This represented a 66 % mass loss of material to obtain the minimum resistivity. Figure 4.2 shows the filled box during the first round. The moisture content is approximately 10 %.

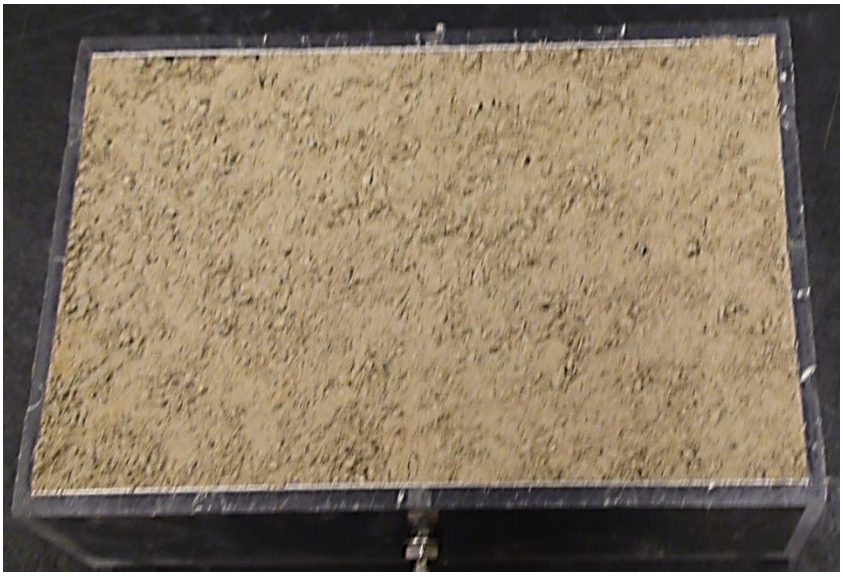

Figure 4.2: Filled AASHTO Resistivity Box (Pittsburg, minus No. 10, w = 10 %)

Figure 4.3 shows the moisture content samples for each of the 13 rounds conducted. The moisture contents increase with each round, so the rounds progress in the figure starting from the top and spiraling clockwise inward until reaching the 13th round represented by the leftmost smaller container. The wet samples filled the containers to the brim; the right picture is tilted to visualize the amount of moisture loss during drying.

Figure 4.3: Moisture Samples for Each Pittsburg Round (Left: Wet; Right: Dry)

Table 4.1 shows moisture content and resistivity of the Pittsburg material used for each round.

Table 4.1: AASHTO T 288 Results (Pittsburg)

	Resistivity			Resistivity	
Trial	Ohm-m	MC %	Trial	Ohm-m	MC %
R1	67.51	9.8	R7	8.84	58.3
R2	20.46	15.6	*R8*	*7.43*	*113 (83*)*
R3	16.07	21.6	R9	7.09	88.0
R4	13.17	26.5	R10	6.89	106
R5	12.09	31.0	**R11**	**6.48**	**128**
R6	9.99	55.1	R12	6.55	138
			R13	6.68	152

* Round R8's moisture content discrepancy may be attributed to an unrepresentative sample because it was difficult to equally collect all representative parts of the resulting slurry. Linear interpolations with respect to both the mass of solids in the box compared with those of R7 and R9 and the resistivity compared with those of R7 and R9 yielded moisture contents of 83.6 % and 82.2 %, respectively. It is thus reasonable to assume that the actual moisture content of R8's material was approximately 83 %, and not 113 %.

The minimum resistivity reported for the Pittsburg material according to AASHTO T 288 occurred in R11, 6.48 ohm-m.

4.1.2: AASHTO T 288 Ridgeview Results

The AASHTO T 288 test was conducted with approximately 1500 g of dry Ridgeview material passing the No. 10 (2 mm) sieve. The minimum resistivity of 6.62 ohm-m occurred at a moisture content of 280 %. The mass of solids compacted in the box in the first round was 1013 g; this number was 217 g by the 12th round, at which the minimum resistance was measured. This represented a 79 % mass loss of material to obtain the minimum resistivity. Figure 4.4 shows the moisture content samples for each of the 13 rounds conducted. The moisture contents increase with each round, so the rounds progress in the figure starting from the top left and continuing to the right for each subsequent row, similar to reading an English book. The wet samples filled the containers to the brim; the right picture is tilted to visualize the amount of moisture loss during drying. Table 4.2 shows moisture content and resistivity of the Ridgeview material used for each round.

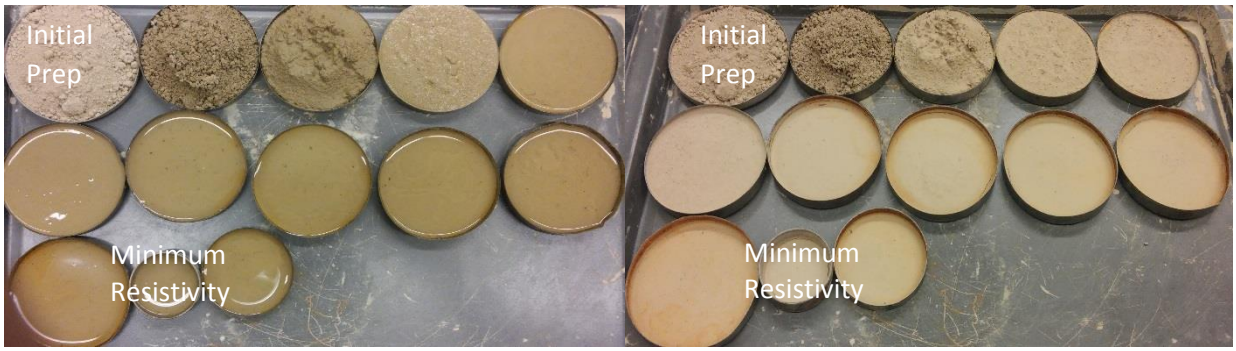

Figure 4.4: Moisture Samples for Each Ridgeview Round (Left: Wet; Right: Dry)

Table 4.2: AASHTO T 288 Results (Ridgeview)

	Resistivity			Resistivity	
Trial	Ohm-m	MC %	Trial	Ohm-m	MC %
R1	>135	1.02	R7	8.78	99.0
R2	48.6	9.16	R8	7.68	73.6
R3	20.2	16.2	R9	6.84	163
R4	17.4	22.0	R10	6.84	210
R5	13.6	30.6	R11	6.74	279
R6	11.7	39.3	**R12**	**6.62**	**280**
			R13	7.24	400

4.1.3: AASHTO T 288 Discussion

According to AASHTO T 288, both the Pittsburg and Ridgeview materials failed to meet the minimum resistivity requirement of 50 ohm-m. Considering the moisture contents of the rounds of interest were over 100 % and 200 %, respectively, this value is unlikely to be representative of field conditions. To represent field conditions, there would have to be in the field a highly segregated (minus 2 mm) pocket of essentially undrainable material in contact with a significant portion of the metal reinforcement. This is unlikely since MSE walls are required to be constructed using free draining and well-mixed backfill material.

Obtaining enough Pittsburg material for AASHTO T 288 required sieving approximately 68 kg (150 lb) of original sample because the fraction of material smaller than 2 mm in diameter was so low. It is possible that the minus 2 mm material had different mineralogy than the larger material rejected from the test sample. Not only was a great deal of sieving required to obtain enough acceptable sample for this test, but the mineralogies of the material passing the No. 10 sieve (2 mm) and the material retained on the No. 10 sieve may have been quite different (shale and limestone). Since limestone is typically more durable than shale, and shale is often found interwoven through the bedrock layers blasted and crushed in the quarry for MSE backfill material, the shale content of any MSE backfill sample is likely overrepresented in the particle size range accepted for this test. Additionally, visual observation of all minus 2 mm material revealed an orange tint regardless of the color of the larger aggregate from the same source material. Thus, testing only the aggregate fraction passing the No. 10 sieve for electrical resistivity testing may bias the sample composition toward weaker materials more prone to breakage and pulverization. Therefore, the tested material may not be representative of the target material.

The AASHTO T 288 resistivity of the Ridgeview material was also reported by Snapp and Kulesza (2015) in their research as 60 ohm-m. This result is much higher than the resistivity of the same material

reported as 6.6 ohm-m in this research. This discrepancy is likely due to a difference in procedure and possibly a material difference between the lab sample and the field-compacted material. The AASHTO T 288 resistivity values reported by Snapp and Kulesza were likely generated using a modified version of the T 288 test which calls for adding water up to and not beyond 100 % saturation, rather than adding water until a minimum resistivity was obtained (which most often resulted in supersaturation and exclusion of a significant portion of the solids from the tested sample) as specified in T 288 and as was done for this project

4.2: New ASTM Results

Since AASHTO T 288 may provide resistivity results based on conditions considered unrepresentative of field conditions, the New ASTM procedure was tested extensively for its repeatability and its field applicability to properly designed and constructed MSE walls with drainable backfill material and no standing water in the backfill.

A total of 69 New ASTM tests were conducted. Often, the smaller box factors of the commercially available boxes (AASHTO and Miller) caused resistance readings to exceed the maximum limit of the AEMC® meter. Therefore, some numerical results for tests using these boxes could not be obtained. This condition represented almost 1/4 of the total number of New ASTM tests conducted, and may reflect an issue that is likely to occur if the ASTM test is used with smaller box factors. Because the resistivity was often significantly higher when measured with the New ASTM test compared with using the AASHTO test, use of the traditional small boxes with small box factors often resulted in resistance values that were too high to be measured with a standard 2,000 ohm ground resistivity meter. For the AEMC® meter used, zero of seven New ASTM tests conducted in the Miller box yielded calculable resistivity results. This problem may be solved using a box with a sufficiently large box factor.

Figure 4.5a shows New ASTM results as a function of box factor. Figures 4.5b through 4.5d show the results as a function of box cross-sectional area perpendicular to electron flow, box volume, and box electrode spacing, respectively. Figure 4.5e shows proposed trendlines based on the data from Figure 4.5d. 'Normal' data points represent tests that followed the New ASTM, i.e. 24 +/-1 hr soaking time of original sample material and use of the AEMC® meter and battery DI water. Deviations from this procedure are noted in the legends and trendlines for each figure where applicable (Figures 6, 7, 10, 13, and 14). The maximum calculable resistivity possible in the AASHTO box was 135 ohm-m (2,000 ohm resistance reading upper limit multiplied by the 0.0675 m box factor), denoted by the blue line near each labeled AASHTO data set. Similarly, the maximum calculable resistivity for material in the Miller box was 12 ohm-m, which is much lower than the required 50 ohm-m KDOT lower limit for MSE backfill.

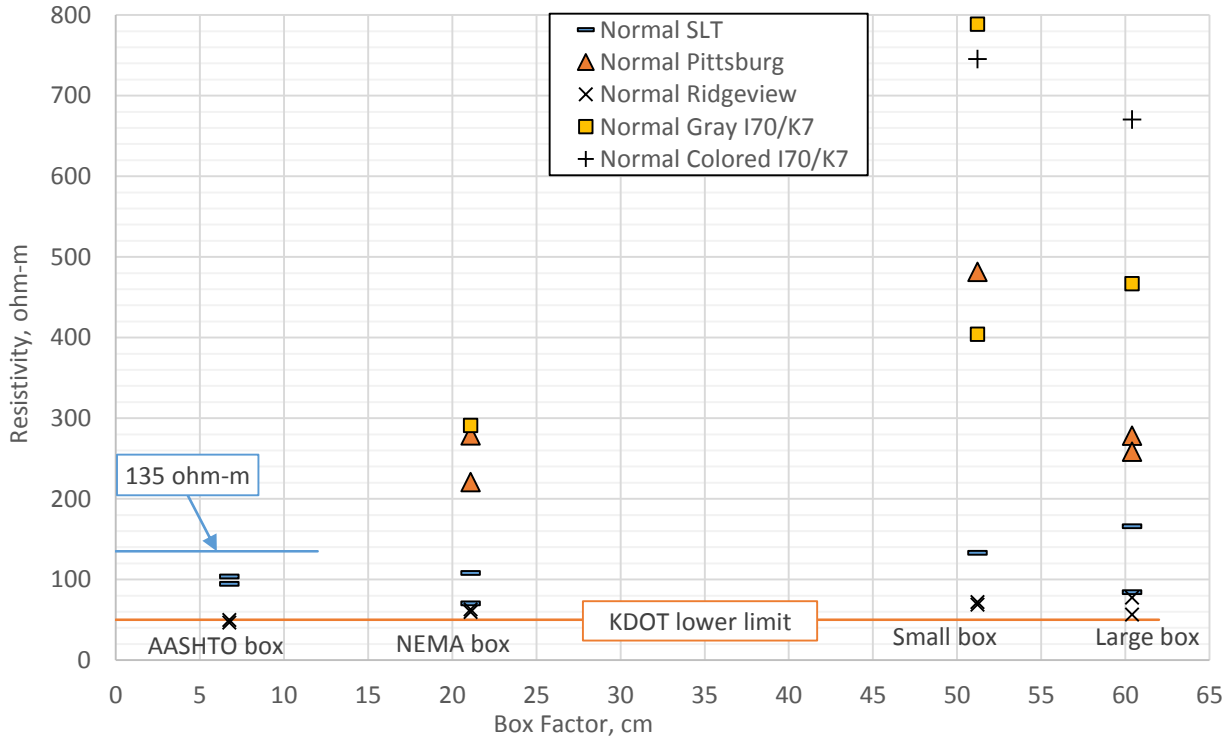

Figure 4.5a: All New ASTM Normal Results vs. Box Factor

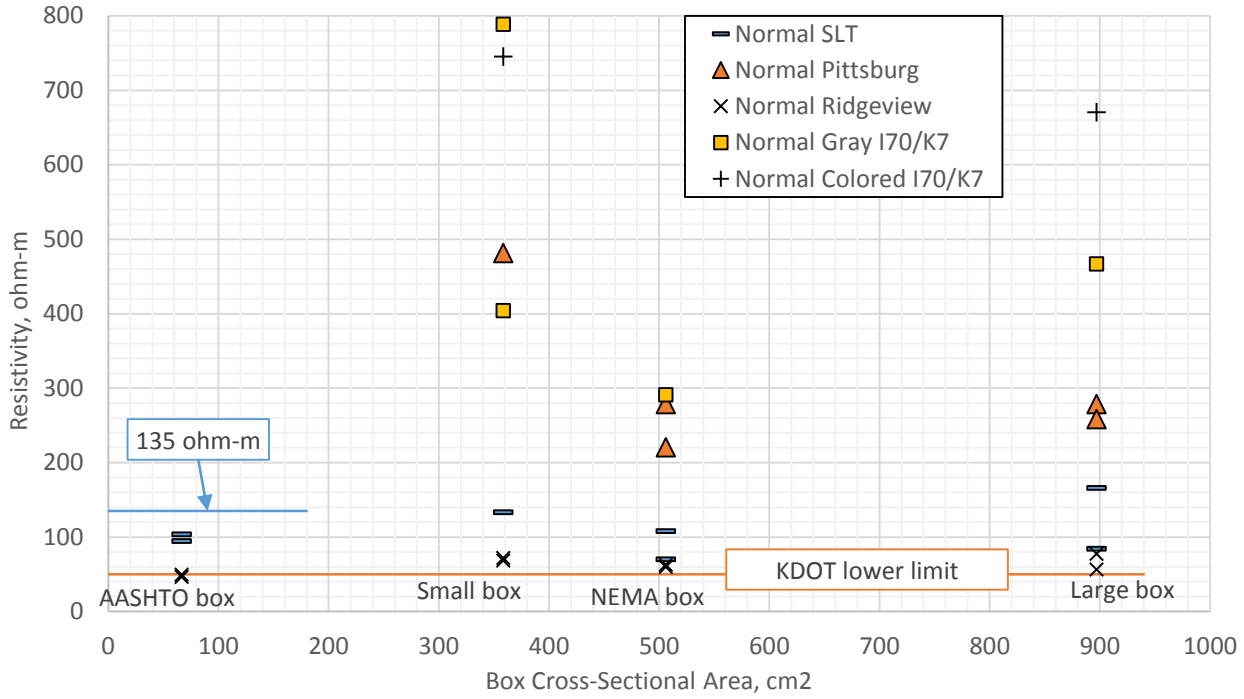

Figure 4.5b: All New ASTM Normal Results vs. Box Cross-Sectional Area Perpendicular to Electron Flow

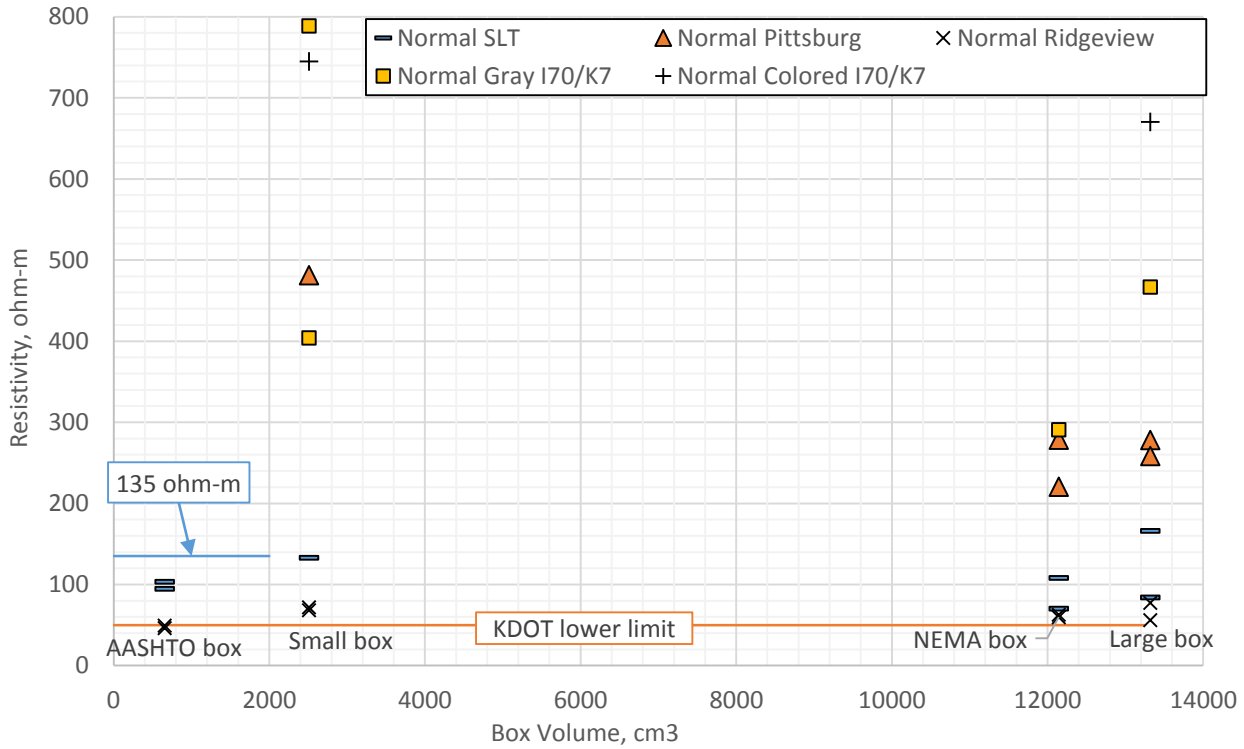

Figure 4.5c: All New ASTM Normal Results vs. Box Volume

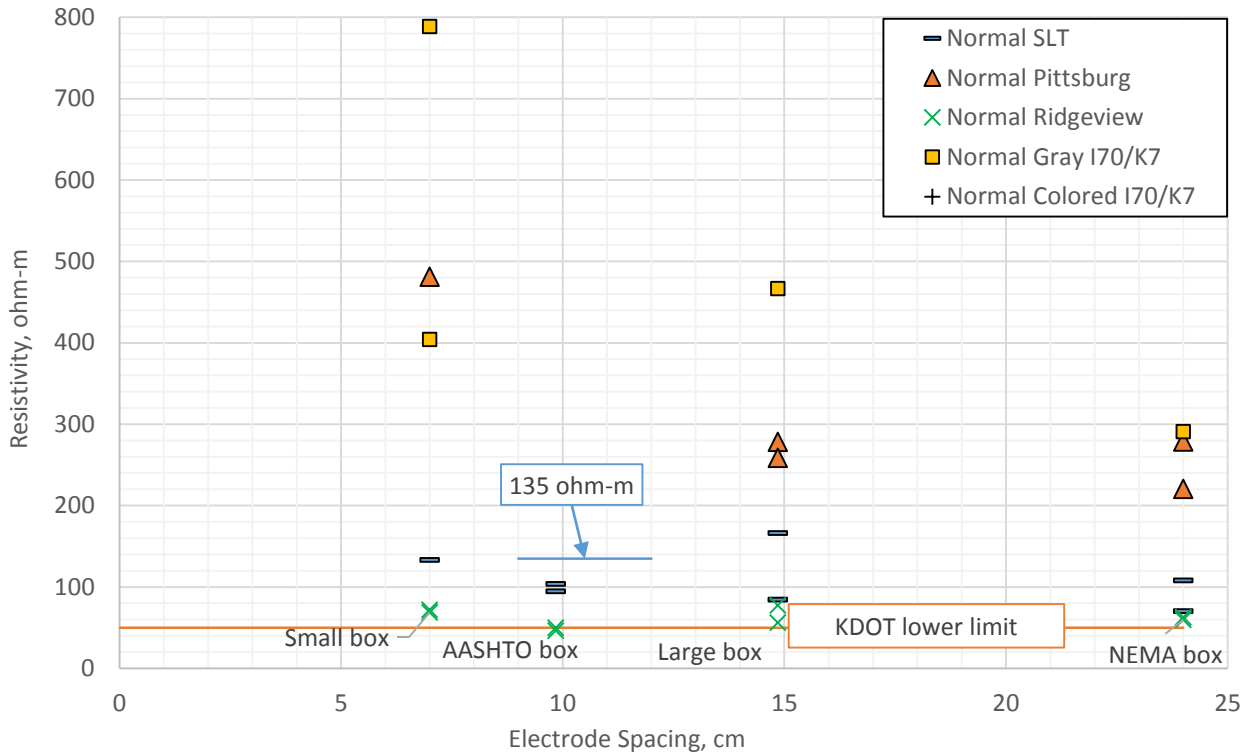

Figure 4.5d: All New ASTM Normal Results vs. Electrode Spacing

Electrode spacing appeared to offer the best correlation, and thus was chosen for display of material-specific results in the following figures. The KDOT minimum resistivity of 50 ohm-m is plotted on each of these figures for y-scale reference. In addition, the KSU field bulk electrical resistivity data (Snapp and Kulesza, 2015) for each material, labeled "Snapp Bulk ER, [value in ohm-m]," are included for comparison. Figure 4.5e displays trendlines based on data from Figure 4.5d. Additional resistivity results with resistivity plotted versus geometric parameters other than box factor are presented in Appendix A.

Snapp and Kulesza (2015) reported both dry and wet bulk ERs for select walls. Where possible, the wet bulk ER was used for comparison with the results obtained in this research for each material due to similar moisture conditions resulting from recently wetted and then gravity drained material. Care must be taken when comparing results from a particular laboratory box to the bulk ER, as the potential exists for there to be variations in moisture content, compaction, mineralogy, and other material properties between the box sample and the bulk-ER-tested compacted backfill.

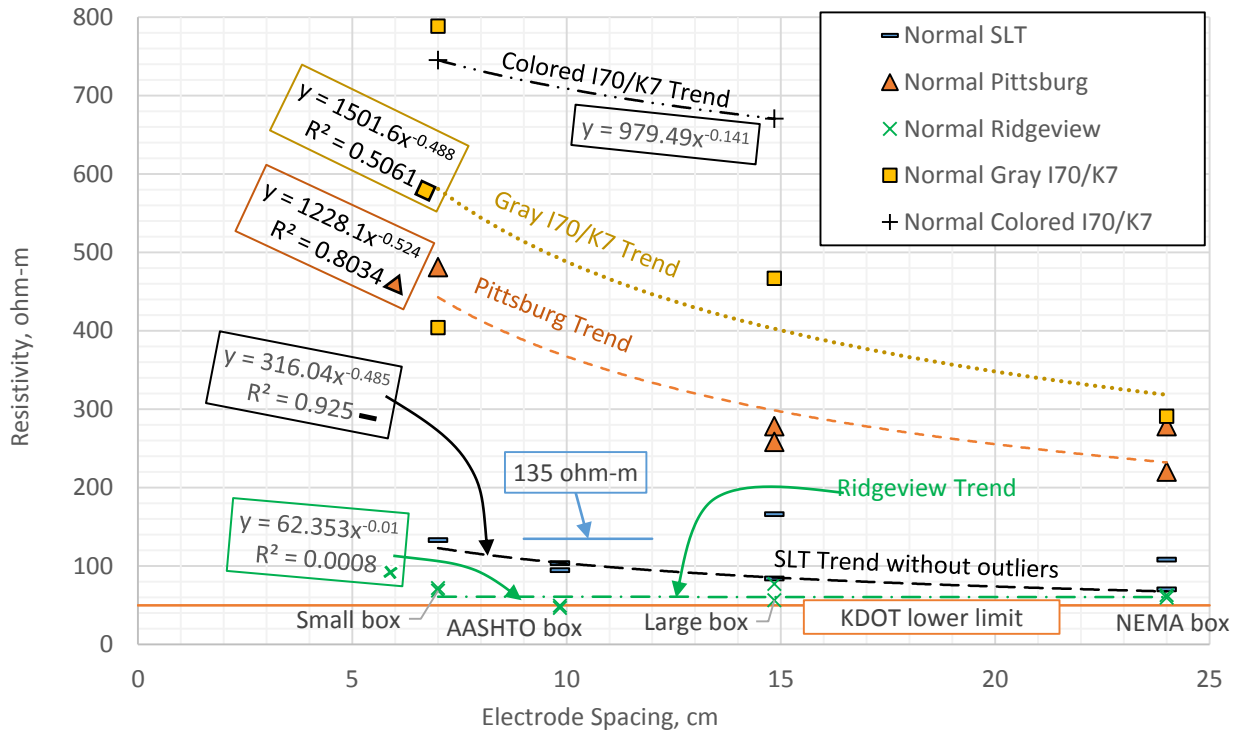

Figure 4.5e: All New ASTM Normal Results vs. Electrode Spacing Trends

It appears from Figure 4.5e that as the electrode spacing increased, both the spread of the resistivity results and their average values decreased. This was most likely due to longer electrical flow paths within the tested material, which tended to reduce the exaggerated effects of larger particle sizes on the electrical flow path length. The larger the ratio of electrode spacing to maximum particle diameter, the fewer electrical flow path distance outliers there may be because the greater distance between electrodes tended to "average out" the effect of very large particles in the electrical flow path.

The majority of Normal material resistivity values in ohm-m exhibited a power law relationship with an approximate exponent of -0.5 with electrode spacing in cm. The colored I70/K7 material may not have been tested enough to verify this power law. The SLT 'outliers' are discussed further in Section 4.2.1 and the Ridgeview data is discussed further in Section 4.2.3.

4.2.1: SLT Material New ASTM Resistivity Results

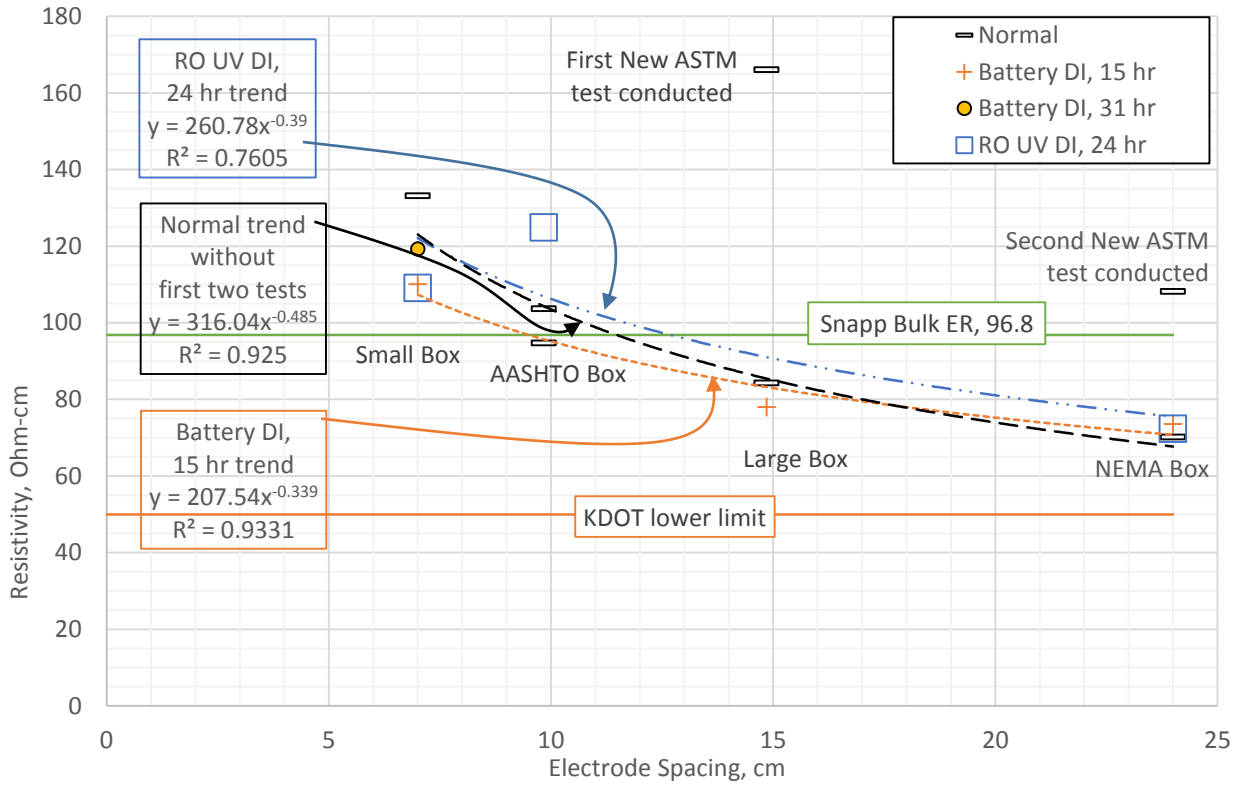

Figure 4.6: SLT New ASTM Results vs. Electrode Spacing

Figure 4.6 shows the resistivity of the SLT material as a function of electrode spacing. The SLT results generally follow the trend of Figure 4.5e with both the calculated resistivity spread and values decreasing as electrode spacing increased, with exceptions being the Large box result over 160 ohm-m and the NEMA result over 100 ohm-m. These were the first two New ASTM tests conducted for this project. Thus, these discrepancies may be due to differing compaction degrees as both the testing style and exact box-filling procedure were still being adjusted to accommodate specific laboratory conditions and equipment. These tests were repeated, and results similar to those for the Large and NEMA boxes using battery DI water were obtained. Considering that the two initial tests may have differed slightly from the others as the procedure, especially regarding compaction, became routine, the NEMA box appears to have given the both lowest and most accurate values of material resistivity regardless of the

soaking time and the water type used. Please note the y-scale differences between Figures 4.5e and 4.6. The decline in resistivity with electrode spacing appeared to taper off for electrode spacings above 20-25 cm (8-10 in). This is approximately 12 times the maximum particle size for this aggregate.

The Normal tests seem to follow the proposed trendline well if the first two New ASTM tests conducted are ignored. The other tests fall within the same range, which suggests that the various adjustments to the New ASTM procedure represented by those other data points have limited or negligible effect on the calculated resistivity.

KSU bulk resistivity field test data for the wet condition is also plotted in Figure 4.6. As shown in the figure, the lab New ASTM data was very consistent with this field resistivity data.

4.2.2: Pittsburg Material New ASTM Resistivity Results

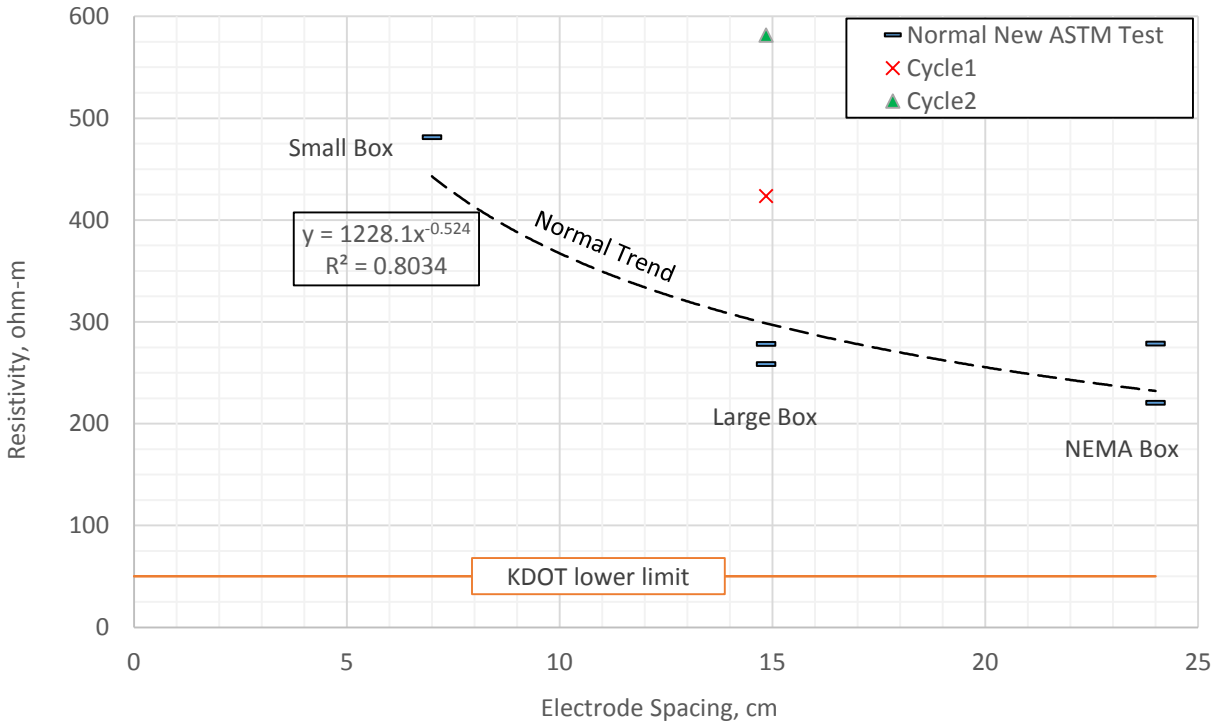

Figure 4.7: Pittsburg New ASTM Results vs. Electrode Spacing

Figure 4.7 shows the resistivity of the Pittsburg material as a function of electrode spacing. As with the SLT material, the Pittsburg material seemed to follow the general trendline set by Figure 4.5e with the NEMA box samples having the lowest resistivity. For this test, the Large box gave the most precise Normal results, represented by the 14.9 cm electrode spacing data. The two higher results (red X and green Δ) represent once- and twice-drained material—different materials than the original Pittsburg material because each soak/drain cycle removed more finer particles from the original sample. Overall, the NEMA box still appears to give the most conservative results. Please take note of the y-scale differences between Figures 4.5e and 4.7. The decline in resistivity with electrode spacing appeared to taper off for an electrode spacing greater than 15-20 cm (6-8 in). This is approximately 7 times the maximum particle size for this aggregate.

4.2.3: Ridgeview Material New ASTM Resistivity Results

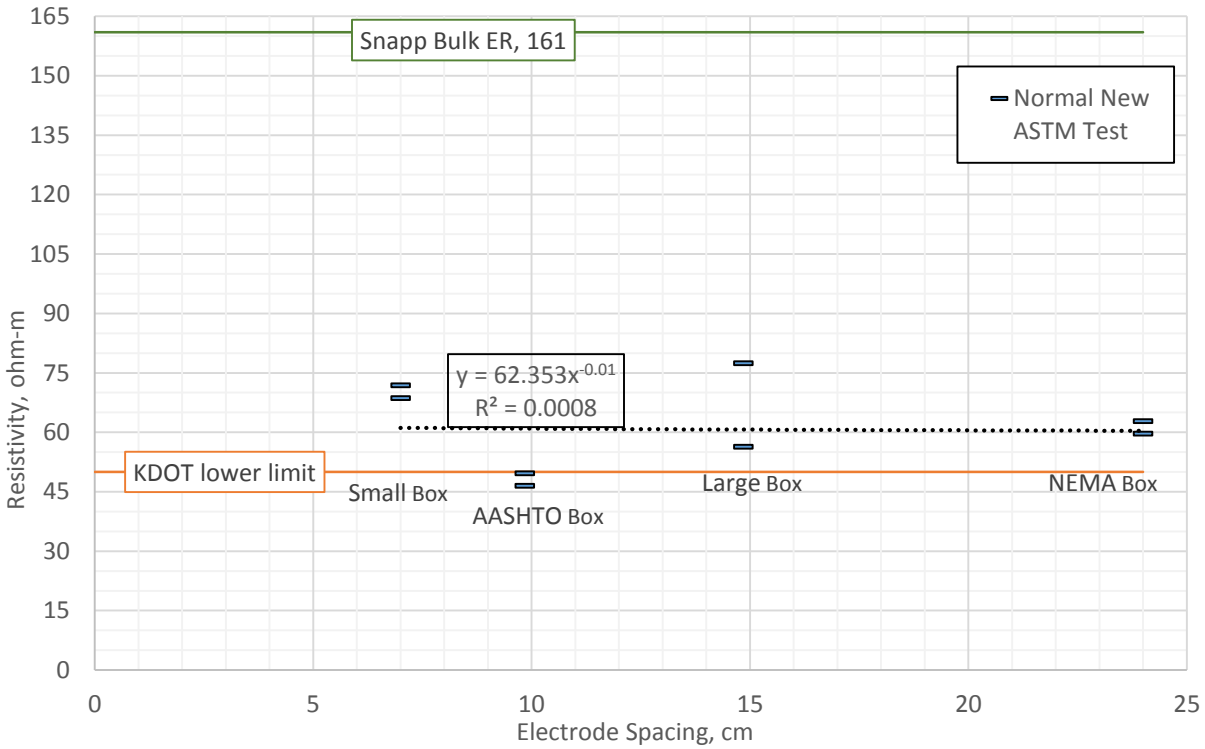

Figure 4.8: Ridgeview New ASTM Results vs. Electrode Spacing

Figure 4.8 shows the resistivity of the Ridgeview material as a function of electrode spacing. The Ridgeview results show that neither AASHTO box sample complied with KDOT specifications for electrical resistivity based on T 288 testing only, and additional testing (sulfates using T 290 and chlorides using T 291) would be required to fully characterize the Ridgeview material prior to acceptance for use as MSE backfill. This particular material failed to drain when the plugs on any of the boxes were removed. This failure to drain was not seen in any other material, which may explain why this Ridgeview data power law fit has such a low R^2 value (essentially zero) compared with the other material data fit curves. The R^2 value indicates that electrode spacing of the test box has virtually no effect on the resistivity of the nondraining Ridgeview material.

In order to obtain the drained resistance readings, a small metal rod was inserted into the open drain hole. After a flow path through the thick layer of finer material blocking the drain was opened, the water level decreased until it reached the finer material layer, at which point drainage slowed to essentially zero. This particle size segregation and drain blocking was seen in all Ridgeview samples tested, and may explain why the Ridgeview material resistivity results were as much as one order of magnitude lower than the results for the other materials. Please take note of the y-scale differences between Figures 4.5e and 4.8. Figure 4.9 shows selected boxes with this 'Ridgeview effect.' This may explain why the Ridgeview material did not seem to follow any discernible trend in Figure 4.8. The Snapp Bulk ER for wet Ridgeview backfill was also much higher than the lab results due most likely to the drainage issue.

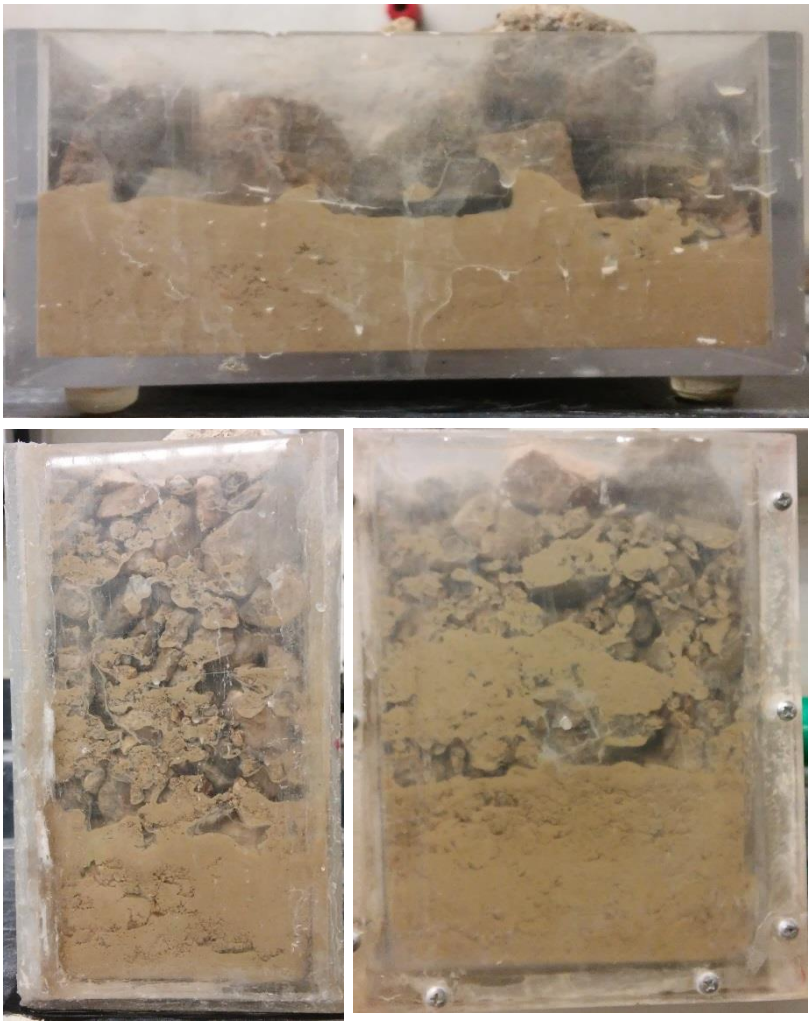

Figure 4.9: Ridgeview New ASTM Samples After Soaking and Attempted Draining: AASHTO Box (top), Small Box (left), and Large Box (right)

4.2.4: Gray I70/K7 New ASTM Resistivity Results SSR8 meter

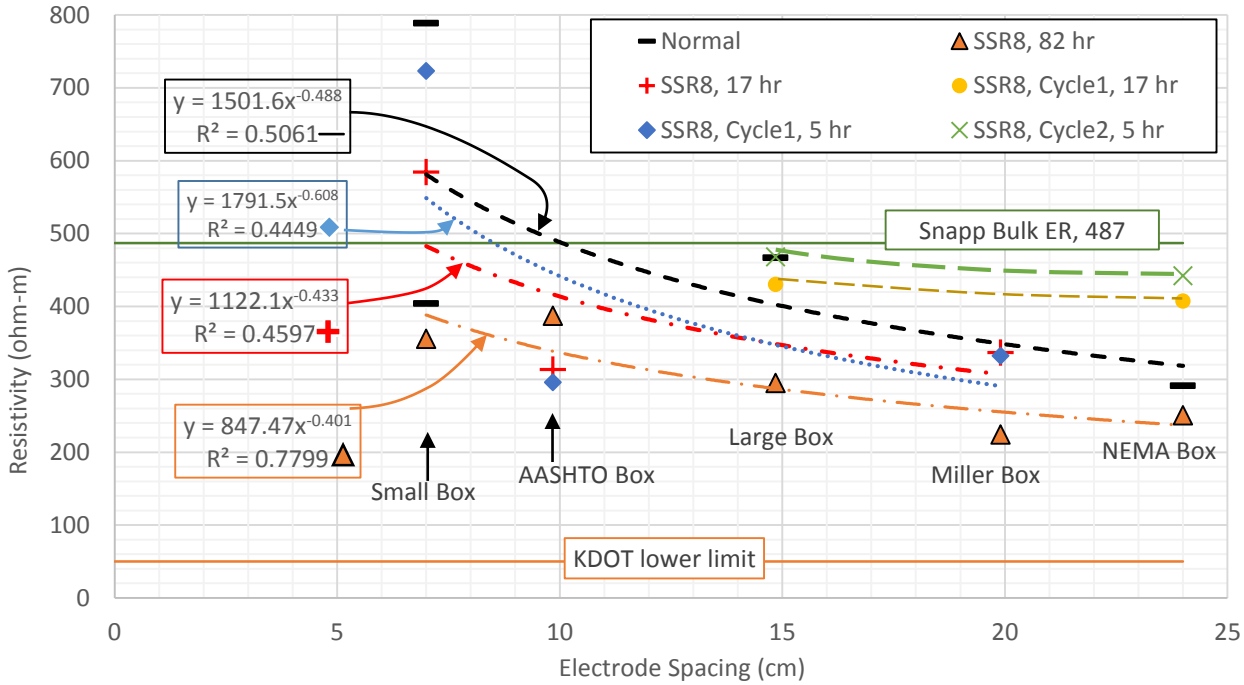

Figure 4.10: Gray I70/K7 New ASTM Results vs. Electrode Spacing

Figure 4.10 shows the resistivity of the Gray I70/K7 material as a function of electrode spacing. The Gray I70/K7 results also generally follow the trend of Figure 4.5e, although with more scatter than previously discussed aggregates. There was a particularly large amount of scatter in the Small box, which had the smallest electrode spacing. The SSR8 resistance values for this aggregate were measured using the SuperSting R8 (SSR8) meter. The Miller box gave similar and relatively precise results compared with the other boxes, most notably compared with the NEMA box, which had consistently been the best thus far. This was not expected due to the small size of the box, which should have reduced test repeatability. For this material, the Miller box appeared to give the most conservative result for the Gray I70/K7 material.

The trendlines also show that calculated resistivity generally decreased with increased electrode spacing regardless of soaking time, type of meter used, or number of soak/drain cycles. The samples

soaked for 82 hours prior to draining appear to have generally lower calculated resistivities than the samples soaked for either 5 or 24 hours. The Snapp Bulk ER for dry I70/K7 material was consistent with the more electrically resistive lab data; this may be attributed to the moisture difference between the freshly drained lab results and the drier compacted field material results.

Most trendlines in Figure 4.10 exhibit an approximate power law pattern with a -0.5 exponent. This suggests that electrical resistivity may be a function of electrode spacing in the boxes, with a different soaking time changing the multiplying constant of the power law to intercept the y-axis at different values. Cycled tests also mostly resulted in higher resistivities. The 5-hour soaked Cycle1 material may not have soaked long enough for direct comparison to the Normal tests regarding the effect of increased soak/drain cycles. The resistivity decline with electrode spacing flattened out for most test procedures at a ratio of approximately 8:1 electrode spacing to maximum aggregate size.

4.2.5: Colored I70/K7 New ASTM Resistivity Results

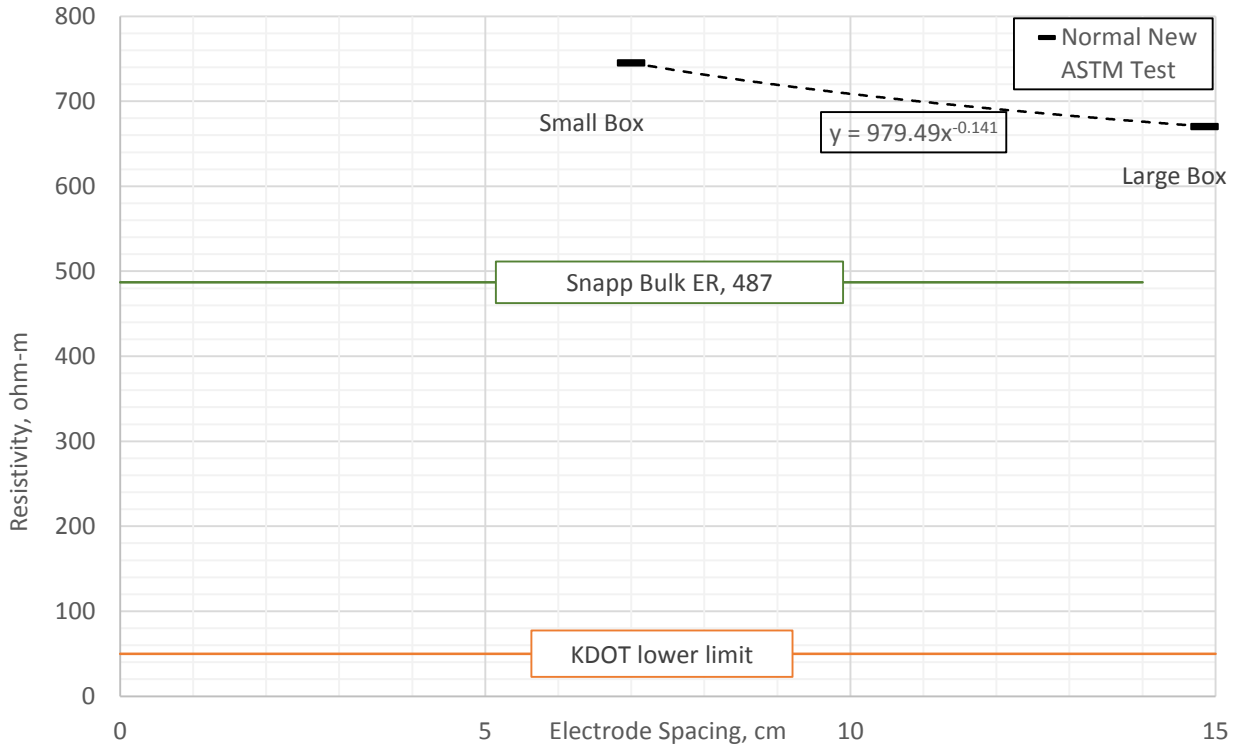

Figure 4.11: Colored I70/K7 New ASTM Results vs. Electrode Spacing

Figure 4.11 shows the resistivity of the Colored I70/K7 material as a function of electrode spacing. Five tests were conducted on the colored I70/K7 material using the proposed ASTM procedure. Resistivity was so high, however, that just two results were obtained due to the NEMA, AASHTO, and Miller box resistance readings overloading the AEMC® meter (box factors of 21.1, 6.8, and 0.61, respectively). The maximum calculable resistivity for the NEMA box was 422 ohm-m. The results still follow the trend seen in Figure 4.5e with respect to increasing electrode spacing lowering the resistivity result. The Snapp Bulk ER for dry I70/K7 compacted backfill resistivity was also very high, but was somewhat lower than either of the data points obtained in the lab.

4.2.6: New ASTM Testing Parameter Variations Results

Figure 4.12 shows the behavior of the calculated resistivity during draining, tilting and draining, and resting after draining for the SLT material in the NEMA and Large boxes. The jumps in resistivity seen at 16 minutes for the Large box and 21 minutes for the NEMA box were due to tilting at those times. The tilt angle for each box was approximately 10° toward the drainage port.

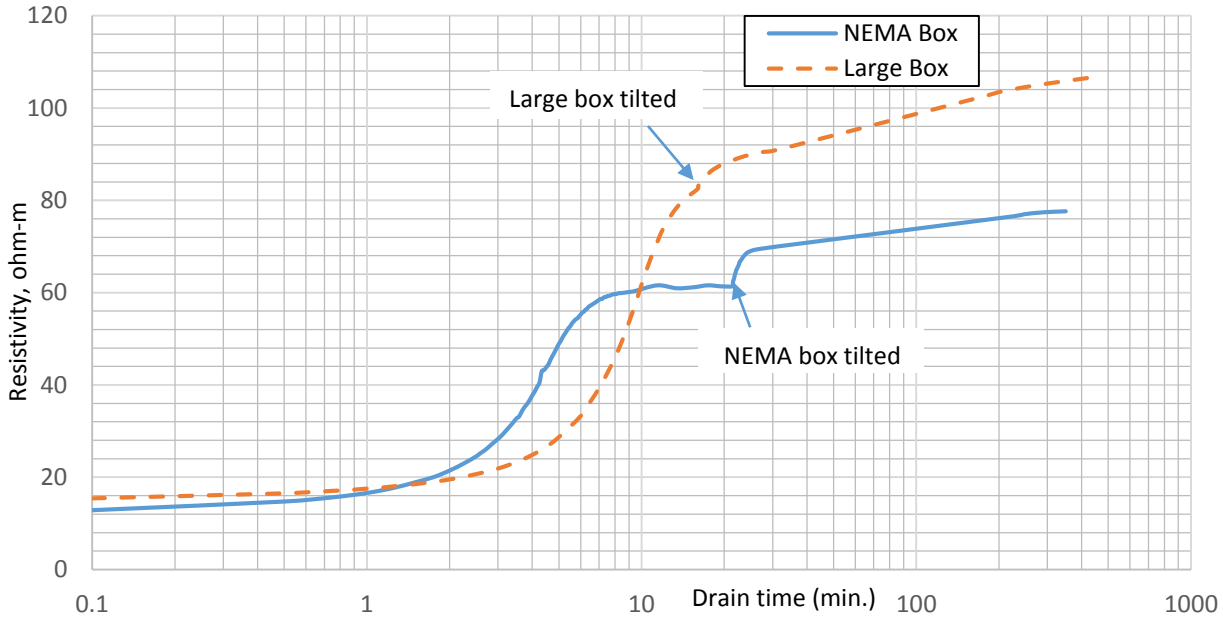

Figure 4.12: SLT Resistivity Behavior During and After Draining

The resistivity increased very slightly for the first few minutes as the boxes drained. It then began to increase rapidly as the water level approached the bottom of the box. An additional increase in resistivity occurred as the boxes were tilted to get the last of the freely draining water out of the box. The flow rate was much higher near the beginning of drainage and the effluent was mostly clear, which may have indicated a lower concentration of suspended sample particles. As the flow rate decreased, the effluent slowly turned a murky brown color, which may have indicated that more suspended solids were leaving the box than just after drainage started. Tilting the box also resulted in similar murky brown effluent. Resistivity continued to increase slightly over the next few hours after complete drainage.

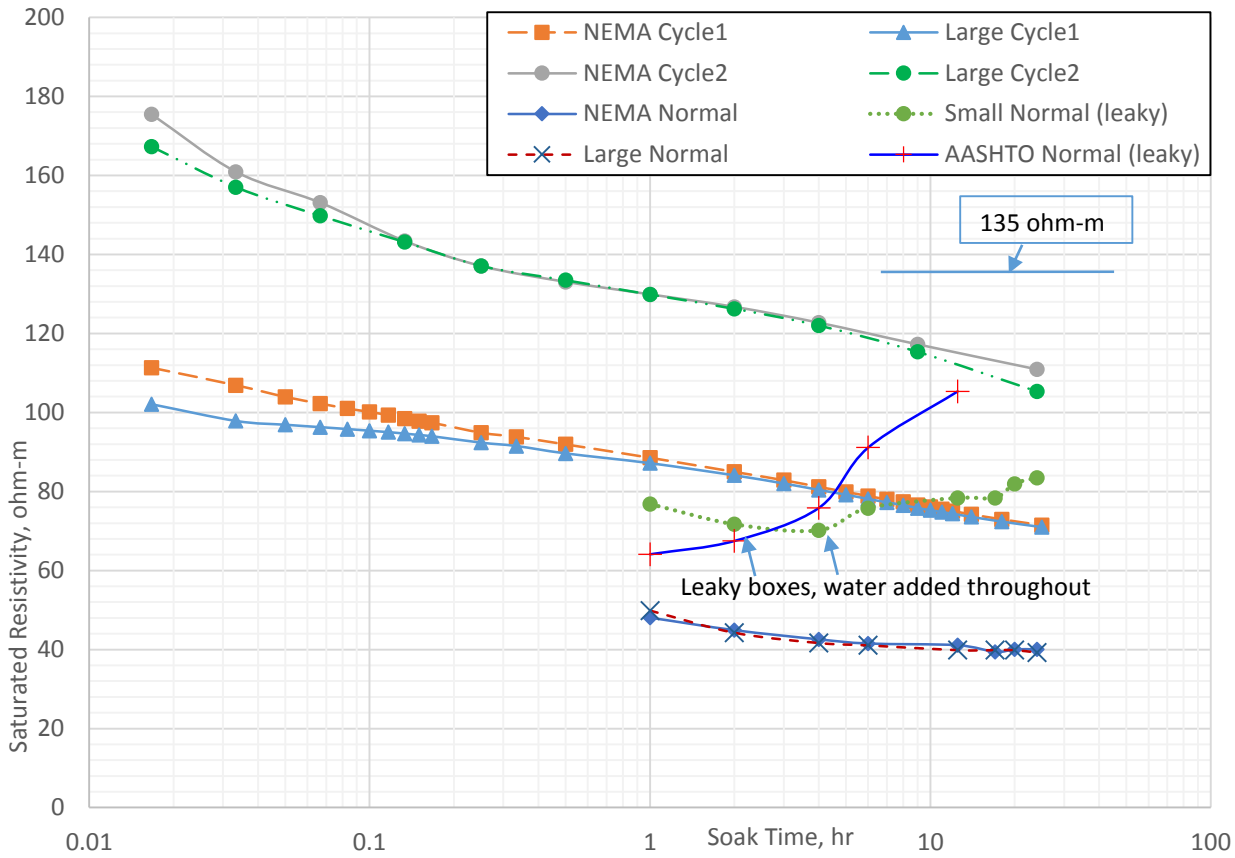

Figure 4.13: Pittsburg Cycled Saturated Resistivity vs. Soaking Time in Different Boxes

Figure 4.13 shows the calculated saturated resistivity changes for Pittsburg and Pittsburg Cycle1 and Cycle2 materials in different boxes as functions of time spent soaking. Figure 4.13 shows a general trend of decreasing saturated resistivity with increasing soaking time for most data. The Large and NEMA box trends offer close correlation of saturated resistivity to the logarithm of soaking time. Equation 1 below models this average correlation. This test was used to investigate the possibility of using a shorter soaking time in the New ASTM and then extrapolating the results to obtain the 24-hour result. This would allow a quick field test to either accept or reject MSE backfill before installation rather than waiting on lab results for a 24-hour test if a saturated standard was adopted.

Both the Small box and the AASHTO box leaked substantially during this test, which required replacing over 1/3 of the water volume for each box after each reading. Every time that battery DI water

was added to these boxes, the resitivity increased. Considering that the added water was deionized, its addition must have diluted the concentration of ions that came from the sample.

Figure 4.14 shows the data from Figure 4.13 without the leaky boxes and with the the drained resistivities of each cycle number of material in the Large box. The NEMA box, with its moderate box factor of 21.1 cm, contained the same material in a shape too electrically resistive to be measured by the AEMC® meter.

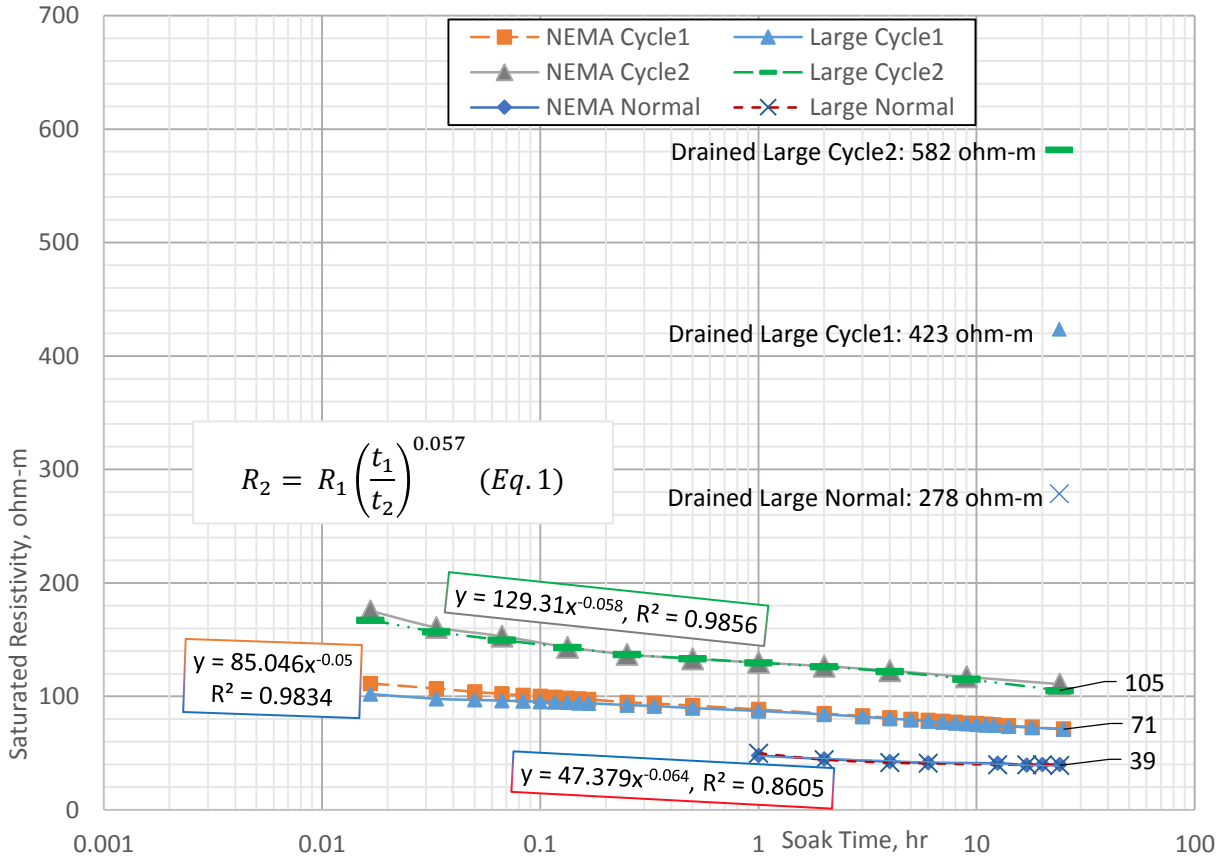

Figure 4.14: Pittsburg Saturated and Drained Cycled Resistivities vs. Soaking Time in Different Boxes

Equation 1 is a best fit relationship for predicting the 24 hour resistivity of Pittsburg material based on any saturated resistivity result with a soaking time between 10 and 1440 minutes and is shown in Figure 4.14 plotted with the data from Figure 4.13. In addition, the similarity of the Large and NEMA results indicated that for saturated resistivity, the degree of repeatability of results across different box

shapes was high, which suggests that these boxes were sufficiently large for box shape to not significantly influence resistivity.

$$R_2 = R_1\left(\frac{t_1}{t_2}\right)^{0.057} \quad (Eq.1)$$

R_2 = saturated material resistivity at desired soaking time (ohm-m)

R_1 = measured saturated resistivity (ohm-m)

t_1 = total soaking time elapsed for which R_1 was measured (hr)

t_2 = total soaking time elapsed for which R_2 is desired (hr)

The saturated resistivity of the Pittsburg material increased substantially as it was drained and refilled and became Pittsburg Cycle1 material, and also as Cycle1 Pittsburg was drained and refilled and became Pittsburg Cycle2 material. Figure 4.15 shows the drained resistivities of each of these different cycled materials.

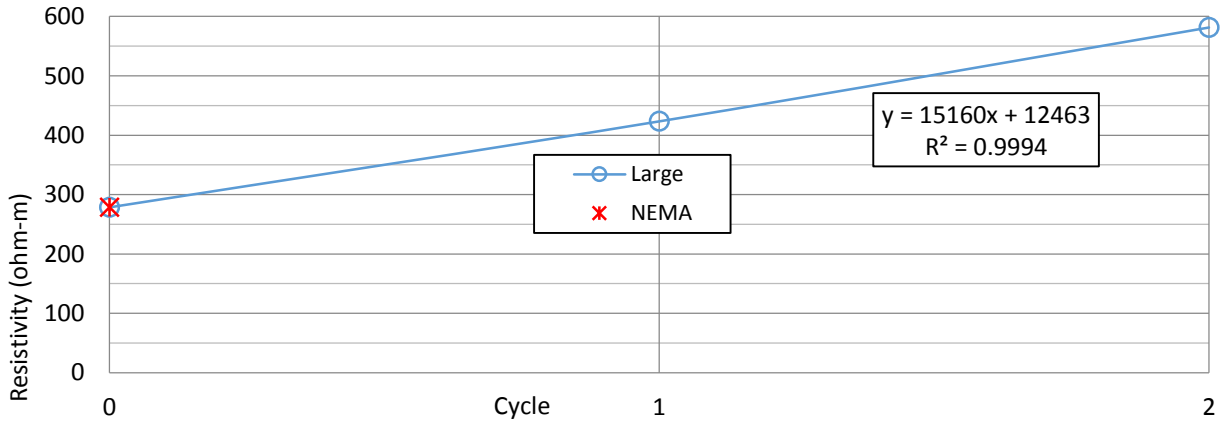

Figure 4.15: Cycled Pittsburg vs. Drained Resistivity (Same Material as Figure 4.13)

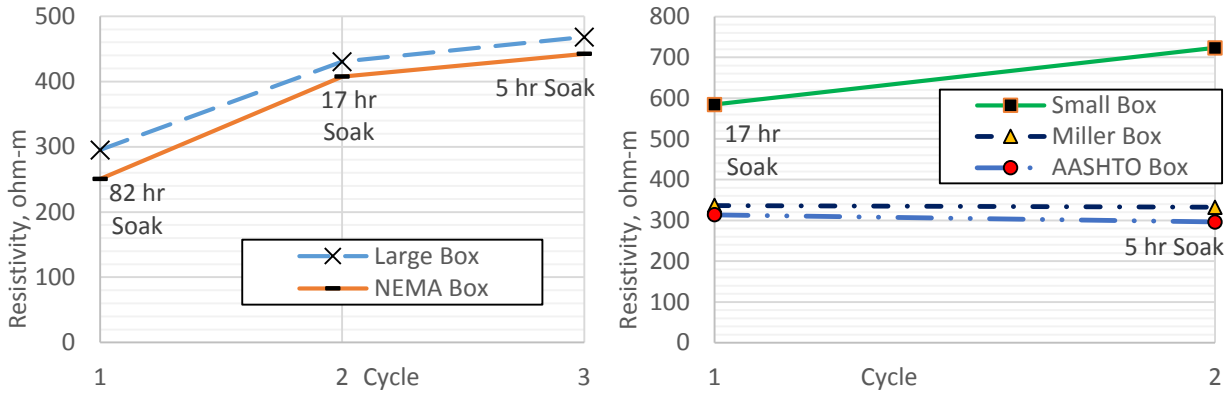

Figure 4.16: Cycled Gray I70/K7 vs. Drained Resistivity

Figures 4.14 through 4.17 show that increasing the number of soak/drain cycles of Pittsburg and Gray I70/K7 material generally resulted in increased resistivity. These cycles were intended to simulate rainfall events followed by drainage of the resulting pore water from the MSE backfill. Since resistivity increased as the number of cycles increased, the lowest resisitivity for aggregate backfill may occur during the first rainfall/drainage event. Subsequent events appeared to result in increased resistivity. As Figure 4.16 shows, resistivity did not increase with increased cycles of Gray I70/K7 material for the two smallest boxes. The reason for the lack of an increase in these small boxes is not well understood. One possible explanation is that this lack of resistivity increase with increasing soak-drain cycles in the Miller and AASHTO boxes may be related to the drainage method (vacuum drained) rather than gravity drainage. Drainage occurred through a much smaller opening and took much longer than for the larger, gravity drained boxes considering the larger amounts of water drainage required for the gravity drained boxes. This may have led to a smaller percentage of fines being removed during the drainage phase.

Longer-term soak/drain cycling tests of both Pittsburg and Ridgeview material indicated that resistivity continues to increase until stabilizing shortly after the 6th cycle for the Pittsburg material and the 7th cycle for the Ridgeview material. Figure 4.17 compares the Pittsburg material data from both this longer-term cycling test and the shorter test shown in Figure 4.15 and with Ridgeview material results.

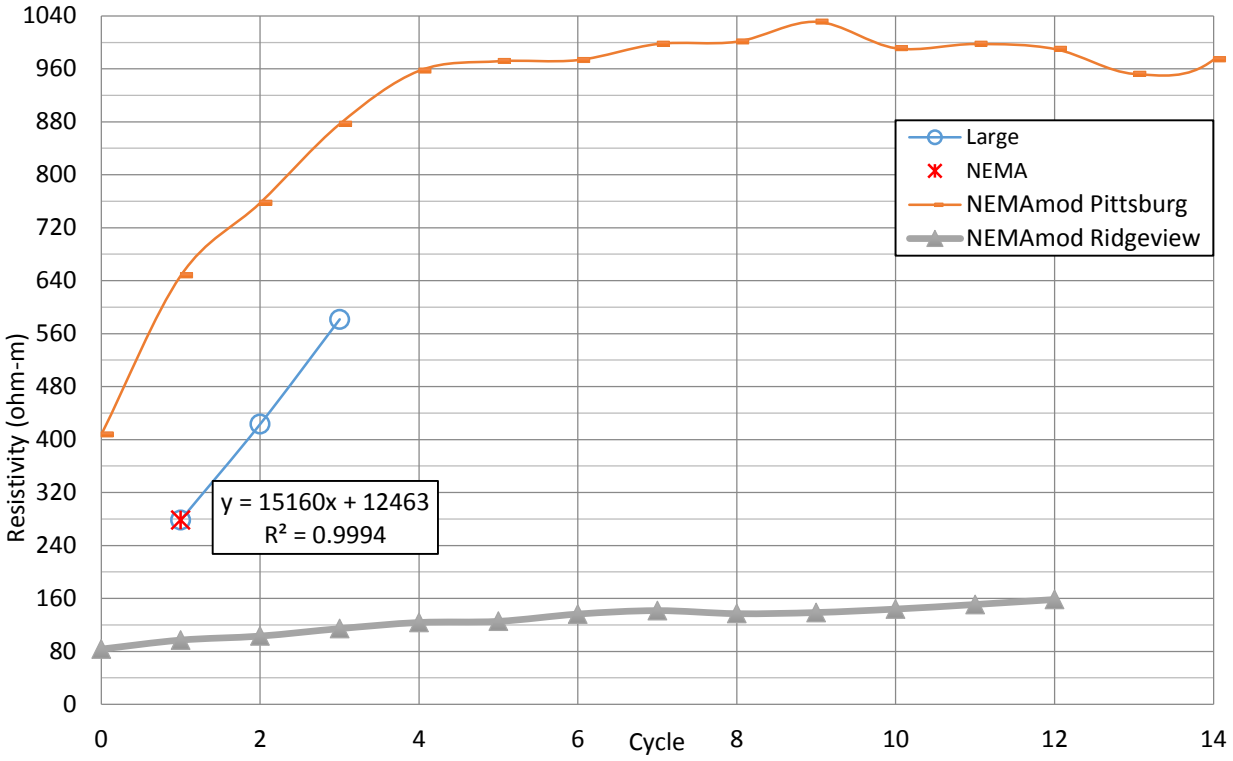

Figure 4.17: Longer-Term Cycled Tests with Drained Resistivity

The drastically lower Ridgeview results may again be attributed to the 'Ridgeview effect,' which affected the degree of drainage compared with the Pittsburg material. Full drainage for these longer-term cycling tests was determined to have been reached when a resistance reading that was stable for at least five seconds was obtained. The approximate full drainage time for each material decreased as the number of soak-drain cycles increased. As soon as full drainage was reached, the drain plug was screwed back in and the next cycle test was prepared immediately. Clear effluent from the longer-term cycle test boxes was observed directly from the drainage apparatus for the entirety of the full drainage process as soon as the resistivity values began to stabilize after the 6th cycle for Pittsburg material and after the 7th cycle for Ridgeview material.

Chapter 5: Conclusions and Recommendations

This thesis contains the results of a research study on the validity of the results of the AASHTO T 288 electrical resistivity test when applied to aggregates used as backfill for MSE walls. This AASHTO test and a proposed alternative ASTM, the New ASTM, test were both used to test a set of aggregate samples obtained from MSE wall construction sites in eastern Kansas. Based on the results of this research, the following conclusions and recommendations were developed.

5.1: Conclusions

5.1.1: AASHTO T 288

Multiple concerns were observed during the AASHTO T 288 tests. These include the maximum particle size limitation that may cause an unrepresentative sample to be tested, the water content of the round of interest (supersaturated) likely to be unrepresentative of field conditions, and the cycling of the sample being tested that results in the loss of a significant percentage of sample solids and likely changes the sample composition to a condition less representative of field material.

The AASHTO test limits the maximum particle size to material passing the No. 10 sieve (2 mm). As Thapalia et al. reported in 2011, limiting an electrochemical test sample to a specific size fraction of an original sample may result in different measured electrochemical properties from those of the original sample. Thus, the limitation of particle size results in calculated resistivities that are representative of the material particles smaller than 2 mm in diameter, but may be unrepresentative of the aggregate as a whole. This tested fraction can be quite small. For the two aggregates tested with the AASHTO method in this study, compliance with the maximum allowable size required sieving 150 lb of each material to obtain the 1500 g of sample necessary to run the test. The most recent update of the AASHTO T 288

standard includes a note referring to the possible lack of validity of the procedure for aggregates with less than 5 % passing the 2 mm sieve.

The AASHTO test often requires testing the aggregate sample in a supersaturated condition. It is unlikely that this condition will occur within significant portions of the backfill behind an MSE wall because MSE backfill is most often designed to be freely draining. Even if this overly saturated condition did exist, the elevated hydrostatic porewater pressures behind the wall would be the main concern regarding failure instead of corrosion. There may be exceptions to this, such as the wall at the K-7 and I-70 interchange designed to permit water flow through the lower portions of the aggregate for periods of time. However, this particular wall has geosynthetic reinforcement.

A third concern with the AASHTO test is the requirement to continue cycling the material by emptying and cleaning the test box, mixing additional water into the sample, pouring all of the resulting slurry back into the box first, then adding sufficient solids back in to fill the rest of the box, and then testing again and again until a minimum resistivity condition is reached. This procedure will change the sample being tested as more and more solids are excluded from the tested portion of the sample during each cycle.

The AASHTO test and its corresponding box were originally designed for use with fine-grained material while the New ASTM test was developed with aggregate samples in mind. Thapalia (2011) was one of the early researchers to question the validity of the AASHTO T 288 method for aggregates. Yzenas Jr. (2014) was one of the early researchers to actually propose a method to estimate the electrical resistivity of these aggregates that the AASHTO test specifically notes as possibly invalid for use with its procedure (i.e. aggregates with less than 5 % passing the 2 mm sieve, See Note 1 in AASHTO T 288). Thus, this research investigated the applicability of the New ASTM proposed by Yzenas Jr. (2014) for use in determining the resistivity of aggregate backfills in field conditions.

5.1.2: New ASTM C XXX-XX

The New ASTM test and the existing AASHTO T 288 standard have considerable differences in procedures and results, and the New ASTM test appears to better represent field conditions for the following reasons:

- The sample is allowed to drain. This should be representative of nearly all MSE wall backfill field conditions, except for special cases as noted previously in Section 5.1.1.
- The full particle size range of the sample is used for the resistivity test and not just the fraction passing the No. 10 sieve (< 2 mm).
- There is not a cycling procedure that results in the exclusion of larger solids from the tested sample.

In addition to the points mentioned above, the box size adequate for the New ASTM will typically be much larger than the AASHTO box. This is important because if the aggregate sample material is to be tested with no particle size restriction then the AASHTO box is almost certainly too small. A single large aggregate particle will often be taller than the AASHTO box and perhaps even span its width, and may therefore dominate current flow, which directly affects resistivity.

Drained samples have a much higher resistance to electrical current flow than their saturated counterparts. The resistance will be higher because the cross-sectional area of current flow is so small due to the reduced number of flow path options for the electrons to traverse the electrode spacing. This resistance is often too high to read using the AASHTO box with the standard meter recommended for AASHTO testing (as was the case for some conditions in this research), and a more sophisticated meter may be required to obtain useful results.

The New ASTM results for electrical resistivity exceeded those for the AASHTO standard by up to two orders of magnitude for the same aggregates. It is likely that this was primarily due to the gravity drained conditions for the New ASTM test versus the supersaturated conditions for the AASHTO test. Larger electrode spacing tended to yield lower resistivity values before leveling off above a certain value that appeared to correspond to the ratio of the electrode spacing to the maximum particle size in the tested sample.

While conducting the New ASTM test on various samples using the different box sizes, several observations were made regarding potential areas of improvement to the procedure.

- The compaction procedure may not have ensured equal compaction efforts among the different box sizes, and so may have rendered the results of each box less comparable to one another for correlation purposes due to differing degrees of compaction and density.
- The lower value of the upper calculable resistivity limit of the Miller box due to its small box factor may limit its applicability to fine-grained soils.
- It may be necessary to develop a different acceptable minimum resistivity of aggregate backfills to use for MSE wall metal reinforcement designs considering corrosion prevention.

It is preferred that the box size be as small as practical for field testing convenience. The similarity of the Large box and NEMA box resistivity curves for each Cycled SLT material provided evidence of the ability to get consistent results from boxes with different shapes. Resistivity generally declined with increasing electrode spacing, although the additional decline above a certain spacing/aggregate size ratio was minimal (12:1 for SLT, 7:1 for Pittsburg, and 8:1 for Gray I70/K7).

Soak/Drain cycling tests were conducted on selected samples. For these tests the appropriately prepared and soaked sample was drained, the resistivity measured, the test box and same sample refilled

with water, and the cycle repeated. This was done in an attempt to simulate the natural process of rainwater cycling through the aggregate. Electrical resistivity increased substantially for these samples with cycling. This suggests that moving water through the backfill may "flush out" some of the constituents that promote electrical current flow, and the resistivity may increase with time and with the number of rainfall then drainage events.

Covering the sample with a sheet of hard plastic while soaking was preferred to plastic wrap with a rubber band. Plastic wrap in contact with the sample and sample water was observed to draw significant amounts of pore water from the top of the sample out of the box via capillary action. For subsequent tests a hard plastic sheet was used to cover each box, and no further capillary action issues were observed.

Saturated resistivity was monitored during the soaking time of select samples, and was shown to decrease as the samples soaked longer, so long as the box did not leak. This was likely due to the extra soaking time allowing more ions to dissolve into the pore solution, which decreases the resistivity of the pore solution and by extension, the bulk resistivity. The saturated resistivity of a longer soaking time for Pittsburg material could be predicted based on a resistivity for a substantially shorter soaking time.

5.1.3: Comparison with Snapp Reported Bulk Field ER

The bulk ER reported for the SLT material was approximately 96.8 ohm-m (wet), which matches very well with the general values of the SLT Normal New ASTM results as shown in Figure 4.6. The bulk ER reported for the Ridgeview material was approximately 161 ohm-m (wet), which is higher than the general results from the Ridgeview Normal New ASTM results. This difference may be attributed to the failure of the Ridgeview material to drain properly via gravity during the New ASTM tests. The bulk ER reported for the combined Gray and Colored I70/K7 materials was approximately 487 ohm-m (dry), which is slightly higher than the New ASTM Gray I70/K7 results and lower than the New ASTM Colored I70/K7 results.

5.2: Recommendations

Based on the research conducted, it is recommended that agencies consider replacing AASHTO T 288 testing with an alternative method, and that the New ASTM procedure be considered for adoption as it better reflects field conditions. It is also recommended that agencies review the resistivity specification for aggregate backfills because it may need to be changed if a drained test is used instead of a saturated (or supersaturated) test.

It is recommended that adoption of a compaction method for the New ASTM similar to the predetermined unit weight method be considered to ensure equivalent compaction degrees across different box geometries.

Based on difficulties in maintaining and water-proofing the edge-to-edge connections in the Small and Large boxes, it is recommended that a New ASTM test box not use silicone to connect or otherwise seal individual box sides. The desired resistivity box should be a single, molded shape of polycarbonate with four seamless sides connected with a seamless bottom and open top. It should have stainless steel electrode plates cut to match the inside dimensions of the desired sides for electrode plate installation and with constant side widths and heights along the sides and bottom of the box. Material types are recommended to conform to the AASHTO standard recommendations for test box material, electrode plate construction, and the fittings required to install the electrode plates and properly connect them to a resistivity meter.

The maximum particle size of the test material is used in the New ASTM to determine the minimum height of an appropriate test box. For this research the electrode spacing seemed to correlate most consistently with the resistivity of the material, and resistivity tended to decrease up to a certain electrode spacing (approximately 20 cm). Based on these results, an 8:1 ratio of minimum electrode spacing to maximum particle diameter is recommended on a preliminary basis. It is also recommended

that the box height complies with the New ASTM recommendation of a 3:1 ratio of minimum box height to maximum particle size. It is also recommended that the box width perpendicular to the electrode spacing be reasonably consistent with the electrode spacing to provide a large number of aggregate contact points and current flow paths to reduce the exaggerated effects of larger particles on electric flow paths.

Based on the preliminary results of the variations of the New ASTM testing parameters, the New ASTM test soaking time may potentially be shortened while still providing accurate results for saturated conditions. Research focusing on the applicability of correlating both the saturated and drained resistivities to soaking time using other MSE backfills is recommended. Further research into the effect of soaking time with more control over other parameters that affect resistivity such as degree of compaction, void ratio and porosity, water content, mineralogy, cementation, tortuosity, and pore fluid resistivity is recommended to accurately determine the minimum adequate soaking time for the New ASTM. Also, it is recommended that additional research be conducted to further explore the tentative relationships identified in this research between electrode spacing and other geometric box factors and resistivity in order to optimize the design of a New ASTM resistivity box.

Further research should also focus on an allowable error in laboratory electrical resistivity test results using a two-electrode soil box as compared with field electrical resistivity test results because the correlated power laws seen in this thesis offer higher repeatability with increasing electrode spacing, but will not mathematically allow for a stabilized result for resistivity, even with infinite electrode spacing.

Recently published research has shown a correlation between the RVE of nondestructive, electromagnetic methods of determining air voids in asphalt pavement and frequency of electromagnetic signal used for the measurement. Asphalt pavement may be a comparable composite material to compacted MSE wall backfill, and electromagnetic measurements may be comparable to electrical

resistance measurements. Thus, this correlation of electromagnetic signal frequency to the required RVE of asphalt pavement electromagnetic property measurement may be applied to aggregate electrical resistivity determinations using a two-electrode soil box. A proper two-electrode soil resistivity box for aggregate backfills, then, should consider the electrical frequency of the resistivity meter used in order to maintain confidence that the laboratory results may be extrapolated to accurately represent the field scale.

References

AASHTO Standard T288. (2012). Standard method of test for determining minimum laboratory resistivity. Washington, DC: American Association of State Highway and Transportation Officials.

American Galvanizers Association (AGA). 2012. "Hot-Dip Galvanizing for Corrosion Protection: A Specifier's Guide." American Galvanizers Association.

Archie, G. E. (1942), The electrical resistivity log as an aid in determining some reservoir characteristics, Trans. Am. Inst. Min. Metall. Pet. Eng., 146, 54-62.

Association for Metallically Stabilized Earth (AMSE). 2006. "Reduced Zinc Loss Rate for Design of MSE Structures: A White Paper and Proposal to Change the Metal Loss Model in the AASHTO Specifications for Design of MSE Walls." Presented to the AASHTO Subcommittee on Bridges and Structures Technical Committee T-15, Substructures and Retaining Walls.

ASTM D75-14. (2014). Standard practice for sampling aggregates. West Conshohocken, PA: ASTM International. doi: 10.1520/D0075_D0075M-14, www.astm.org.

Beckham, Tony L., Leicheng Sun, and Tommy C. Hopkins. 2005. "Corrosion Evaluation of Mechanically Stabilized Earth Walls." Kentucky Transportation Center Report KTC-05-28/SPR 239-02-1F.

Billings, Daniel A. 2011. "Assessing Corrosion of MSE Wall Reinforcement for I-15, Salt Lake County, UT." Brigham Young University Master of Science project. ©Daniel A. Billings, 2011.

Castillo, Carlos, Jesus Hinojos, Aturo Bronson, Soheil Nazarian, and David Borrock. 2014. "Relating Corrosion of Mechanically Stabilized Earth Reinforcements with Fluid Conductivity of Backfill Soils." Transportation Research Board Annual Meeting 2014 Paper #14-3204.

Edlebeck, John E. and Bryan Beske. 2014. 'Identifying and Quantifying Material Properties That Impact Aggregate Resistivity of Electrical Substation Surface Material." *IEEE Transactions on Power Delivery.* Vol. 29, No. 5, October 2014.

Elias, Victor. 2000. "Corrosion/Degradation of Soil Reinforcements for Mechanically Stabilized Earth Walls and Reinforced Slopes." Federal Highway Administration Report FHWA-NHI-00-044.

Escalante, E., "The Effect of Soil Resistivity and Soil Temperature on the Corrosion of Galvanically Coupled Metals in Soil," Galvanic Corrosion. ASTM STP 978. H. P. Hack, Ed., American Society for Testing and Materials, Philadelphia, pp. 193-202.

Esser, Alan J. and John E. Dingeldein. 2007. "Failure of tieback wall anchors due to corrosion." *Geotechnical Special Publication,* Issue 159. Proceedings of Sessions of Geo-Denver 2007 Congress: Case Studies in Earth Retaining Structures (GSP 159). Accession No. 20073610803617

Hazreek, Z A M, M Aziman, A T S Azhar, W D Chitral, A Fauziah, and S Rosli. (2015). The Behaviour of Laboratory Soil Electrical Resistivity Value under Basic Soil Properties Influences. IOP Conf. Series: Earth and Environmental Science 23 (2015) 012002. doi: 10.1088/1755_1315/23/1/012002.

Low, George P. 1895. "Electrolysis and rail-bonding." *Transactions of the American Institute of Electrical Engineers.* American Institute of Electrical Engineers.

Oldfield, J. W., "Electrochemical Theory of Galvanic Corrosion," Galvanic Corrosion, ASTM STP 978, H. P. Hack, Ed., American Society for Testing and Materials, Philadelphia, 1988, pp. 5-22.

Pellinen, Terhi, Eeva Huuskonen-Snicker, Pekka Eskelinen, Pablo Olmos Martinez. (2015) "Representative volume element of asphalt pavement for electromagnetic measurements." *Journal of Traffic and Transportation Engineering (English Edition)*, Volume 2, Issue 1, February 2015, Pages 30-39, ISSN 2095-7564, http://dx.doi.org/10.1016/j.jtte.2015.01.003.

Romanoff, Melvin. 1957. "Underground Corrosion." Circular 579. United States Department of Commerce, National Bureau of Standards. U. S. Government Printing Office, Washington, D. C.

Snapp, Michael A, Stacey Kulesza. 2015. "Electrical Resistivity Measurements of Mechanically Stabilized Earth Retaining Wall Backfill." Kansas State University. Retrieved from <http://krex.k-state.edu>.

Thapalia, Anita, David M. Borrock, Soheil Nazarian, and Jose Garibay. 2011. "Assessment of Corrosion Potential of Coarse Backfill Aggregates for Mechanically Stabilized Earth Walls." *Transportation Research Record: Journal of the Transportation Research Board,* No. 2253 pp. 63-72.

Thornley, John D., Raj V. Siddharthan, Barbara Luke, and J. Mark Salazar. 2010. "Investigation and Implications of Mechanically Stabilized Earth Wall Corrosion in Nevada." *Transportation Research Record: Journal of the Transportation Research Board,* No. 2186, pp. 154-160.

Vilda III, William S. 2009. "Corrosion in the Soil Environment: Soil Resistivity and pH Measurements." Corrpro Companies, Inc. for the National Cooperative Highway Research Program (NCHRP).

Yzenas Jr., John J. 2014. "New Standard 'Coarse Aggregate Resistivity Using the Two-Electrode Soil Box Method.'" WK 24621. To ASTM Sub-Committee C-09.20 Members. Designation: C XXX-XX.

Appendix A: Resistivity vs. Geometric Factors Other Than Box Factor

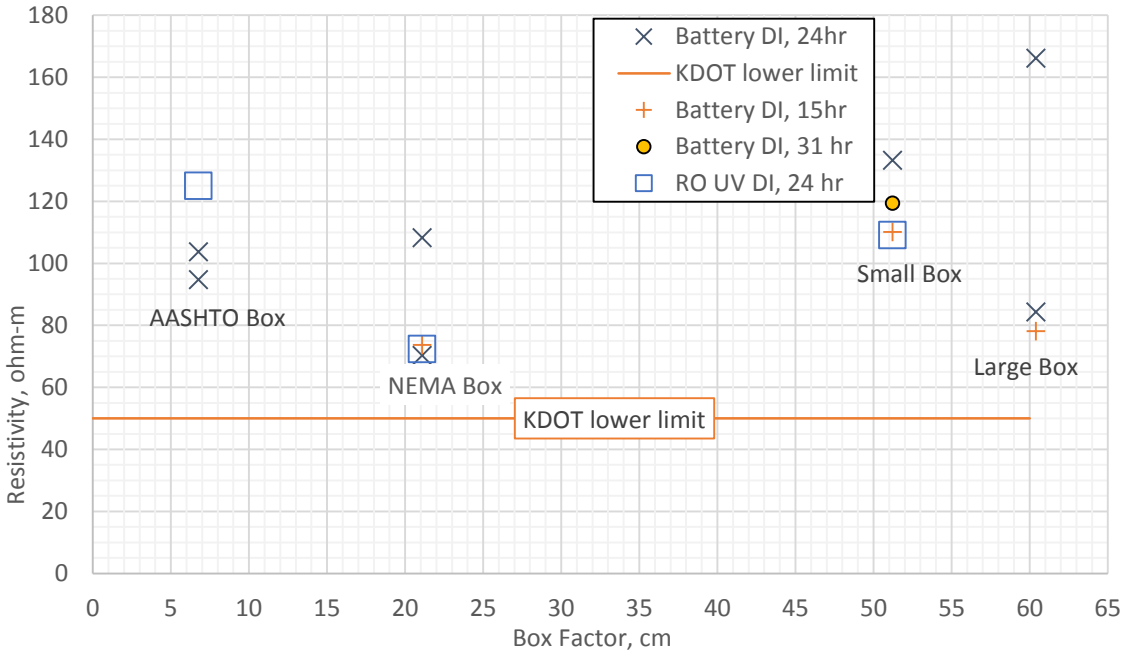

Figure A.1: New ASTM SLT Resistivity Results vs. Box Factor

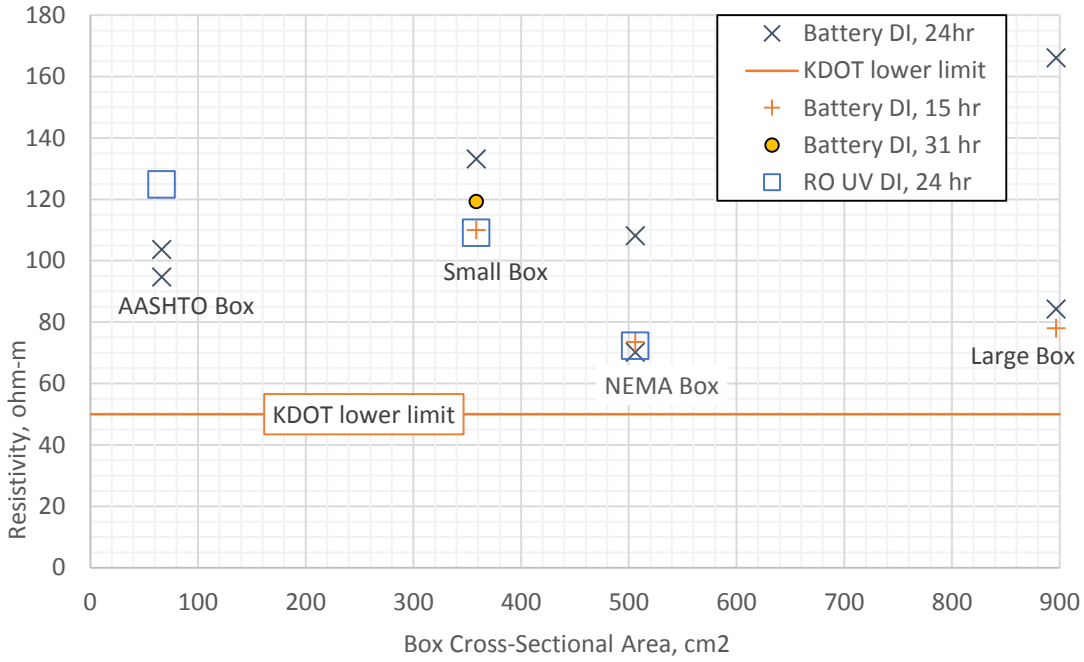

Figure A.2: New ASTM SLT Resistivity Results vs. Box Cross Sectional Area

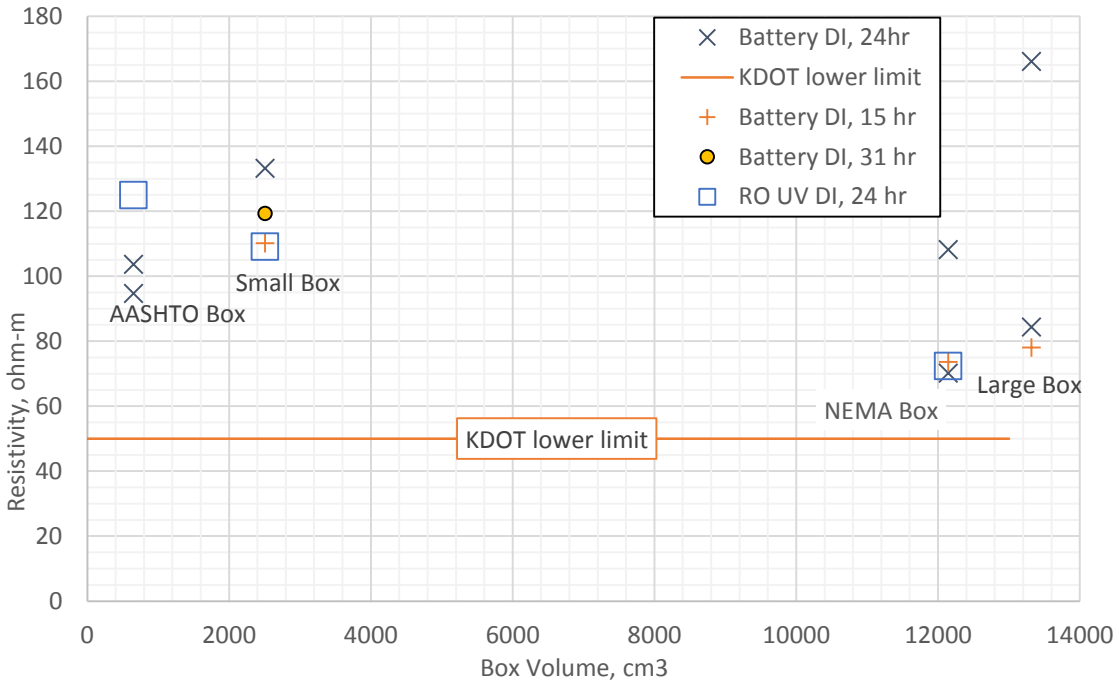

Figure A.3: New ASTM SLT Resistivity Results vs. Box Volume

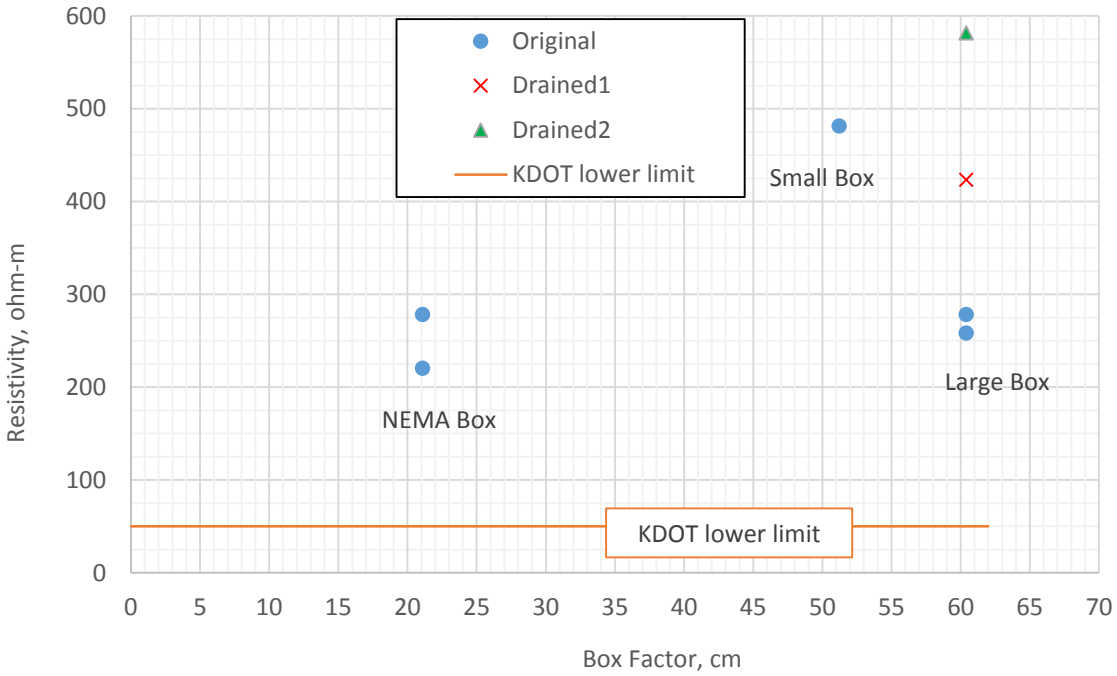

Figure A.4: New ASTM Pittsburg Resistivity Results vs. Box Factor

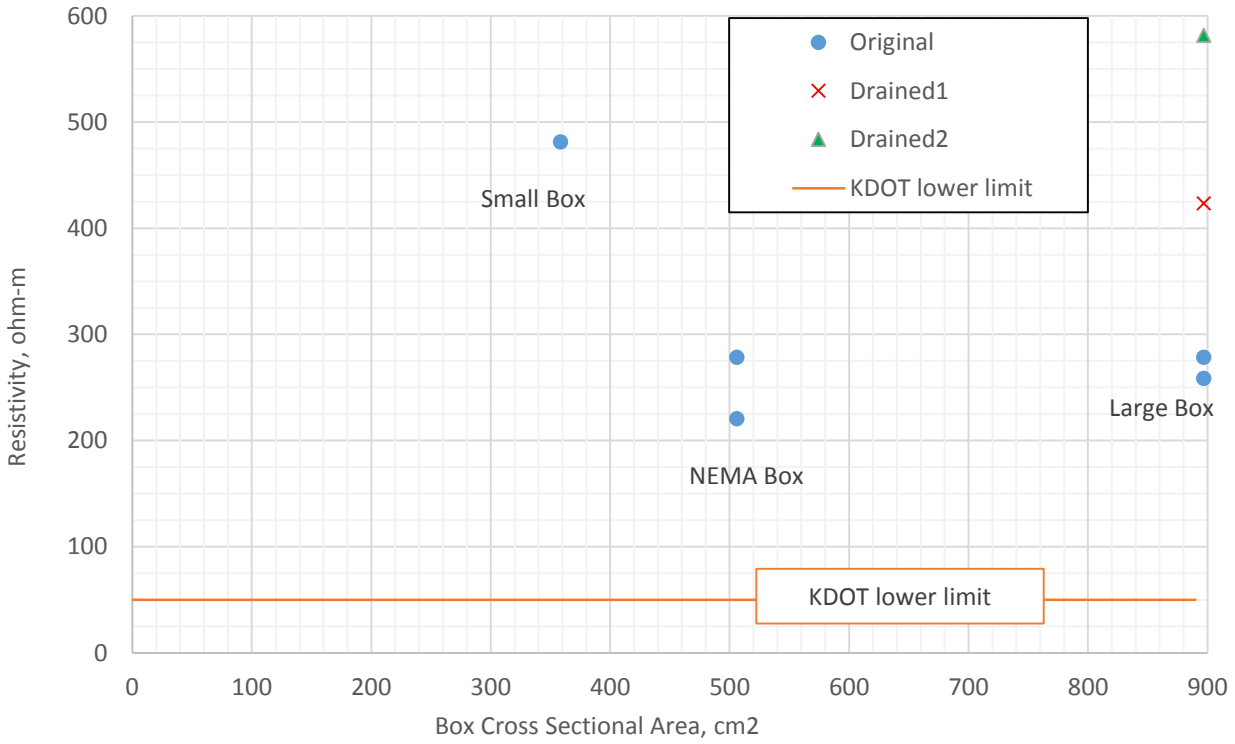

Figure A.5: New ASTM Pittsburg Results vs. Box Cross-Sectional Area

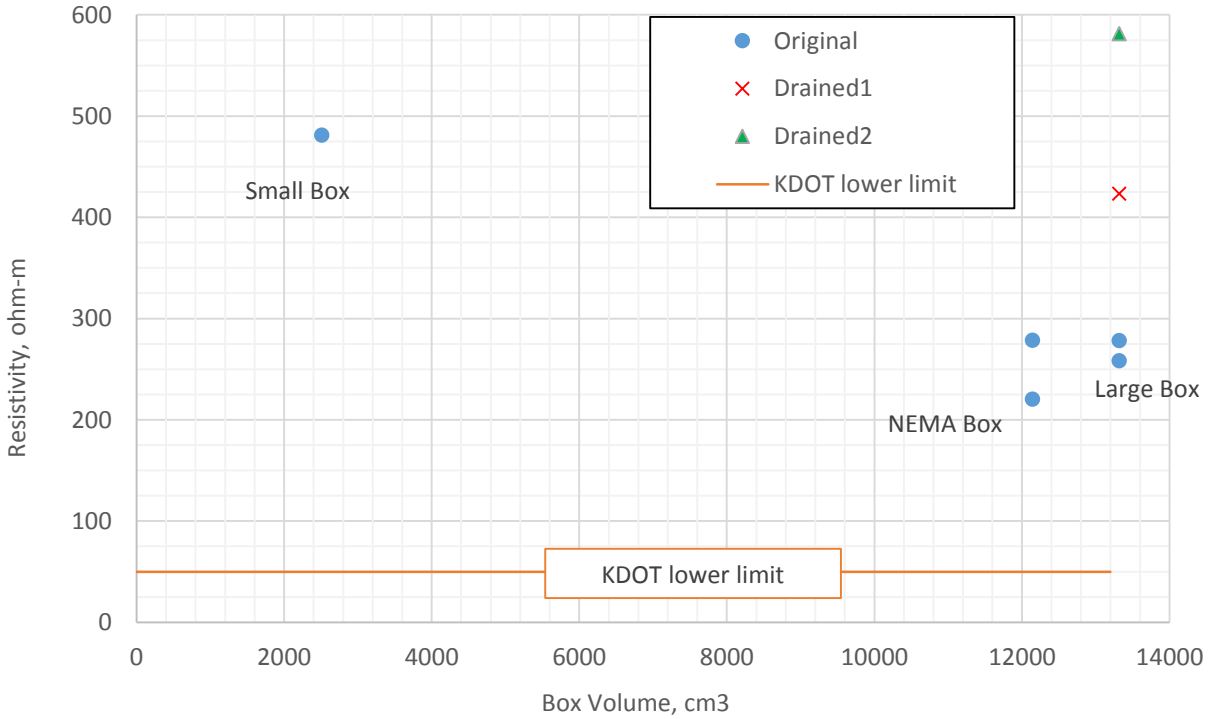

Figure A.6: New ASTM Pittsburg Results vs. Box Volume

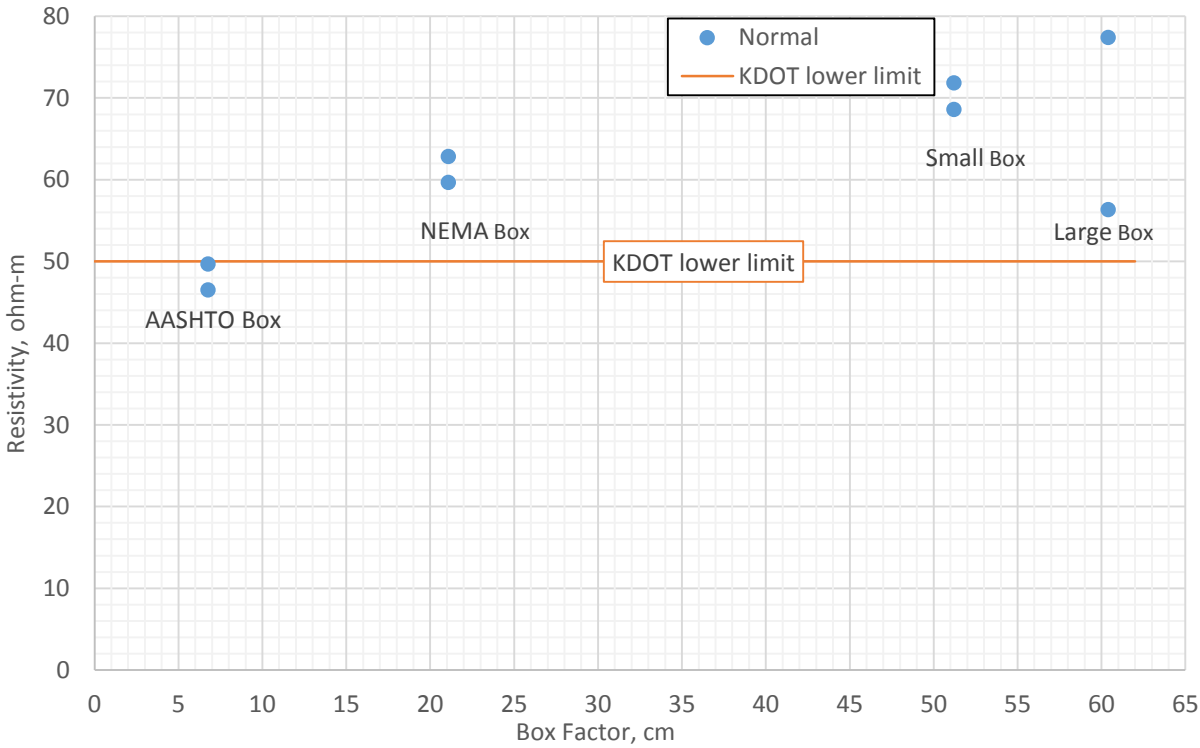

Figure A.7: New ASTM Ridgeview Resistivity Results vs. Box Factor

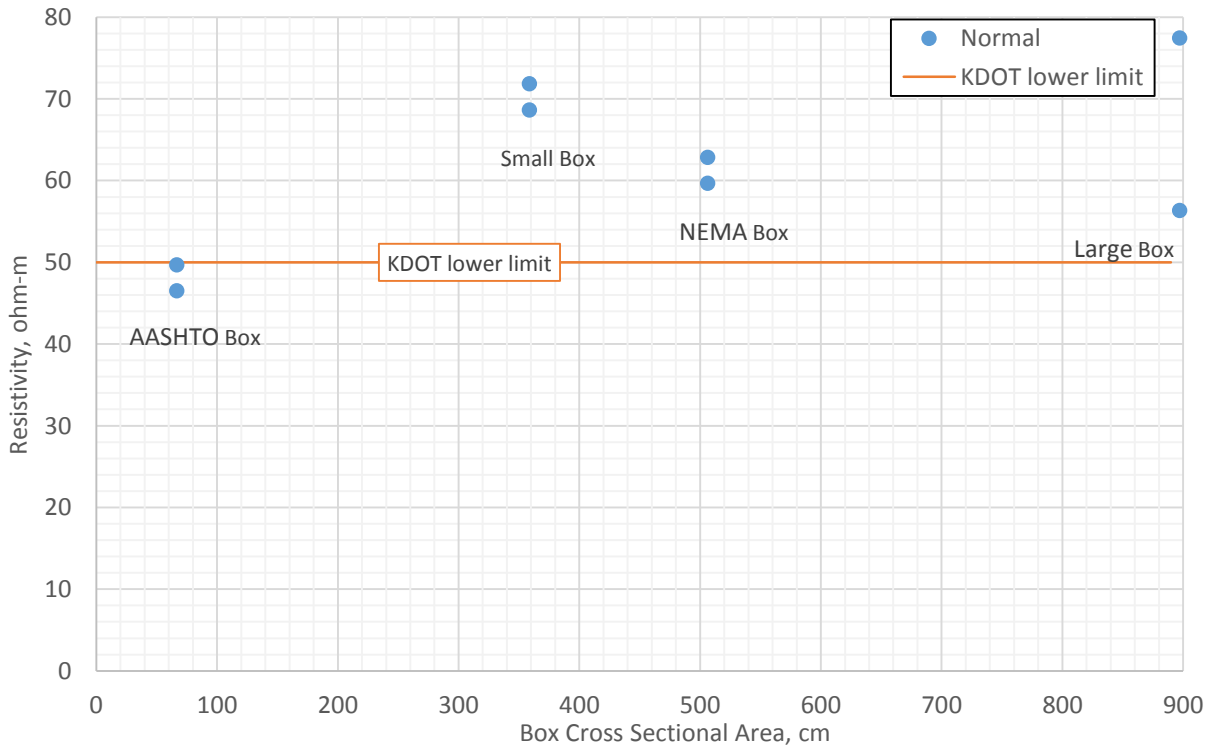

Figure A.8: New ASTM Ridgeview Resistivity Results vs. Box Cross Sectional Area

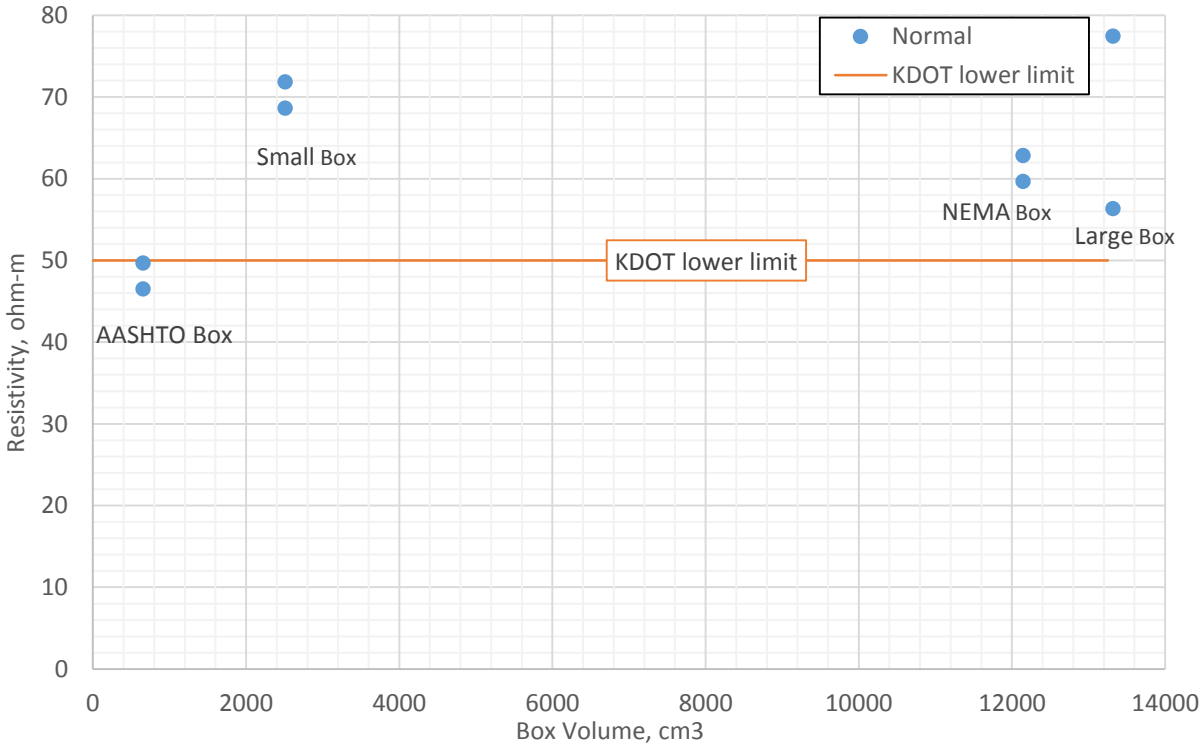

Figure A.9: New ASTM Ridgeview Resistivity Results vs. Box Volume

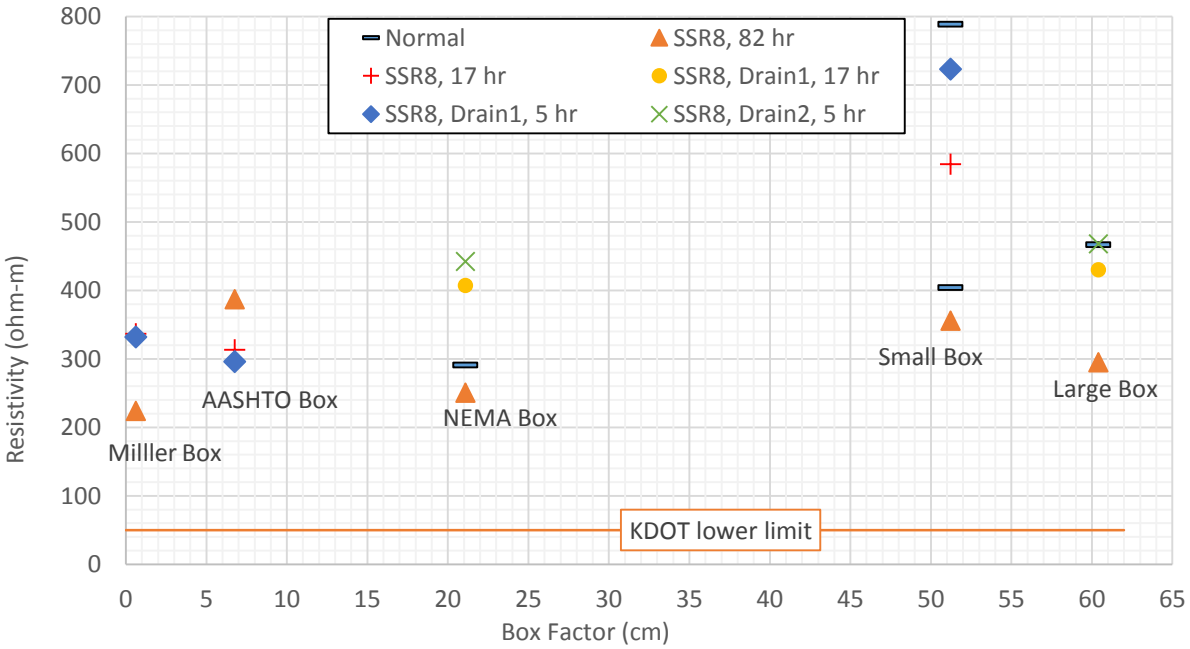

Figure A.10: New ASTM Gray I70/K7 Resistivity Results vs. Box Factor

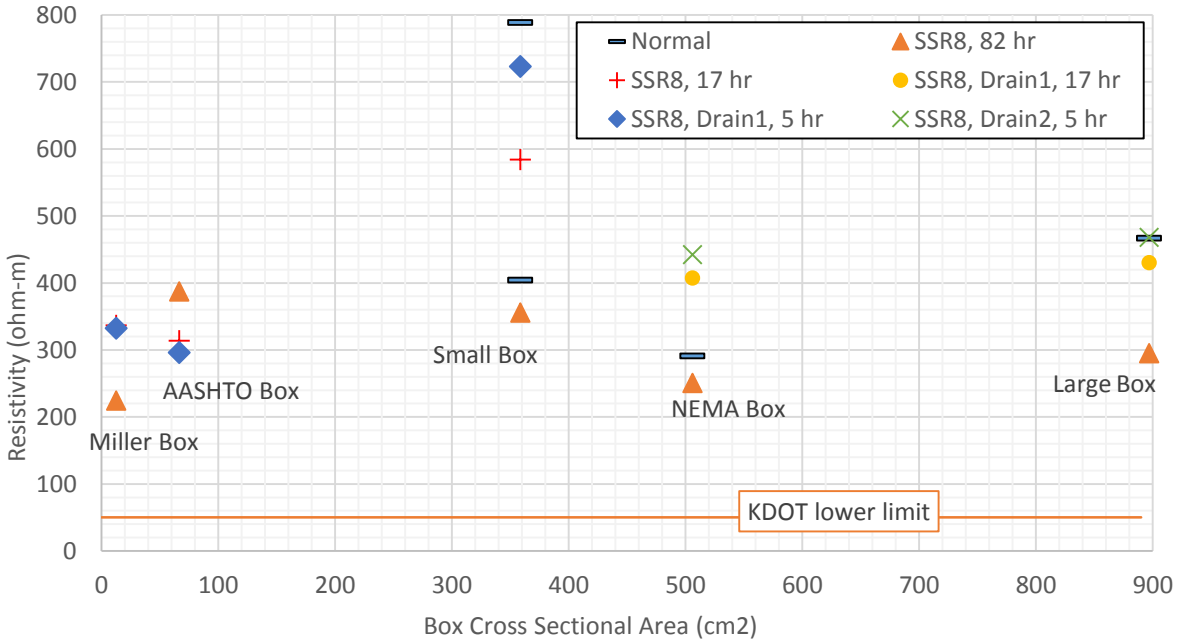

Figure A.11: New ASTM Gray I70/K7 Resistivity Results vs. Box Cross Sectional Area

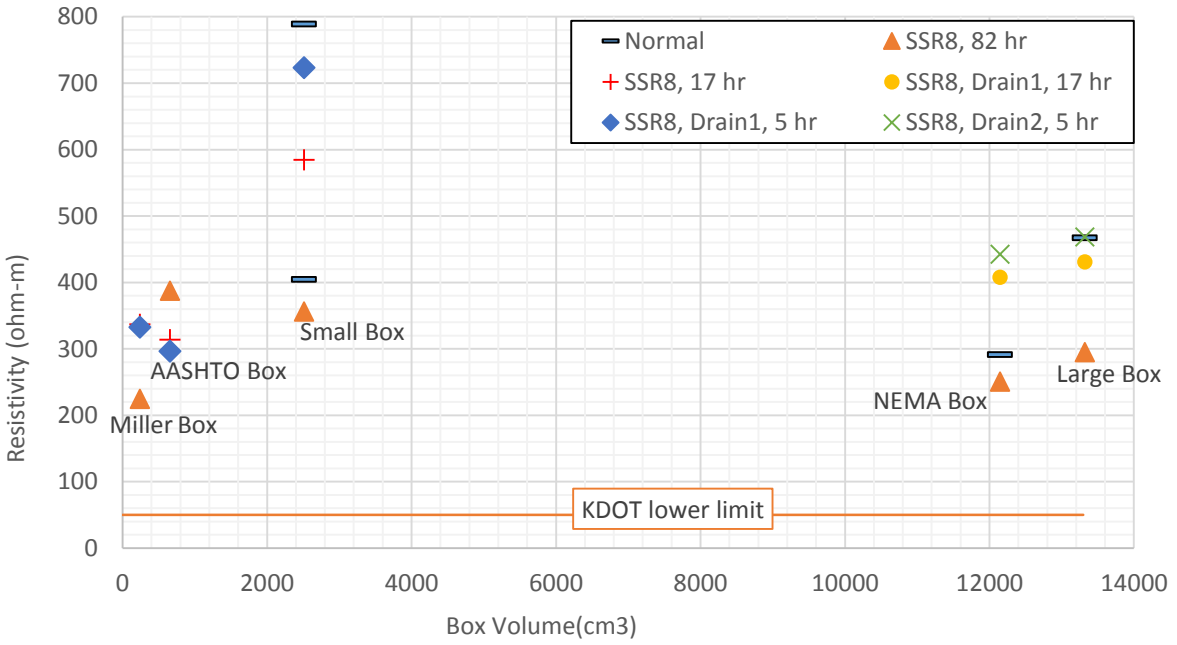

Figure A.12: New ASTM Gray I70/K7 Resistivity Results vs. Box Volume

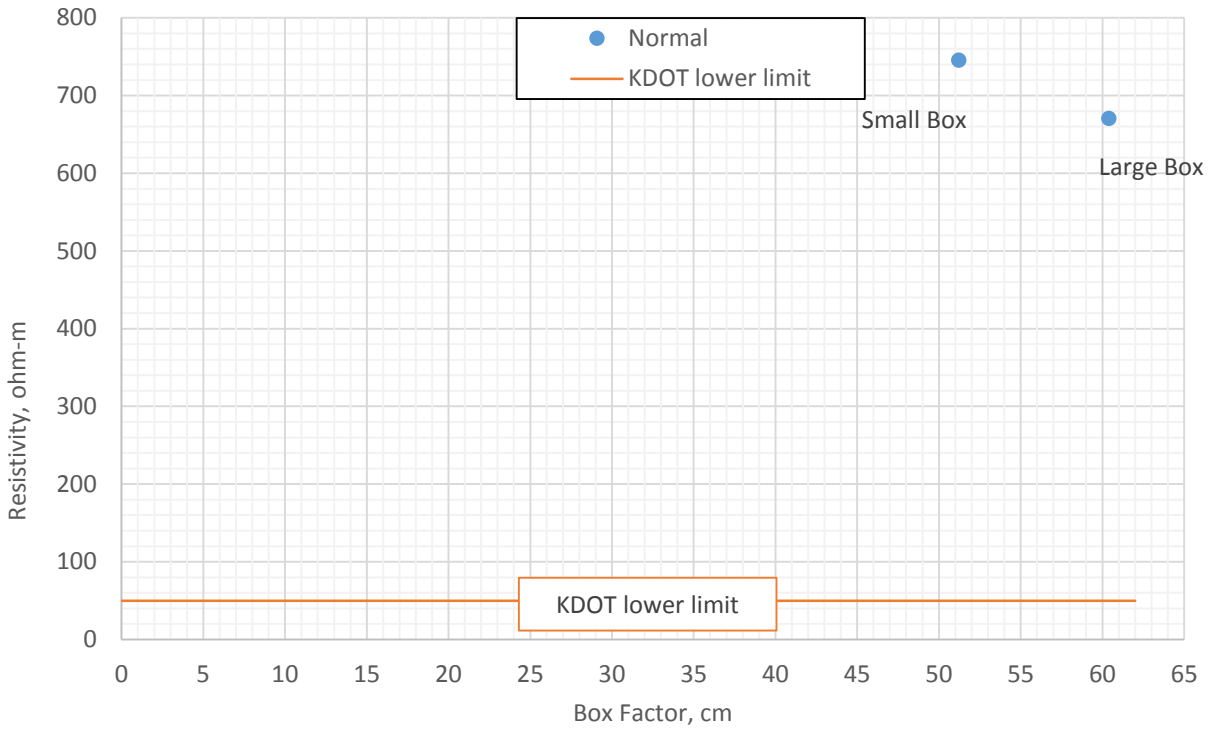

Figure A.13: New ASTM Colored I70/K7 Resistivity Results vs. Box Factor

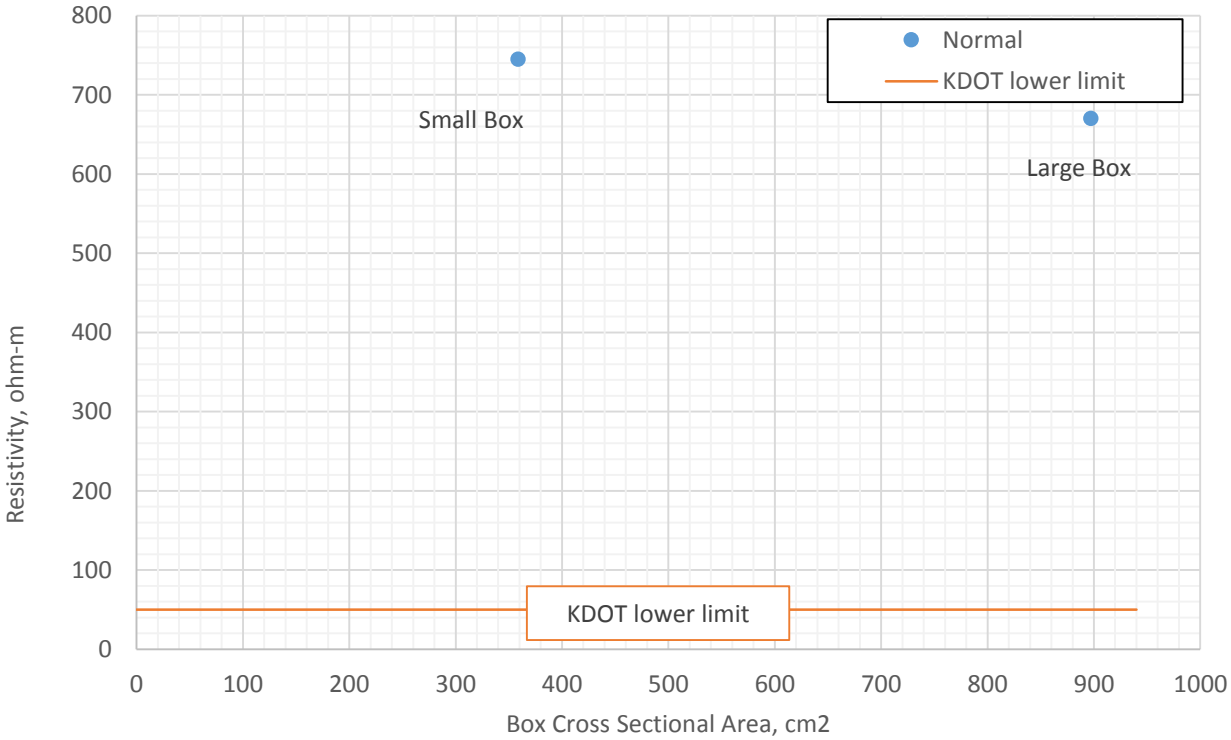

Figure A.14: New ASTM Colored I70/K7 Resistivity Results vs. Box Cross Sectional Area

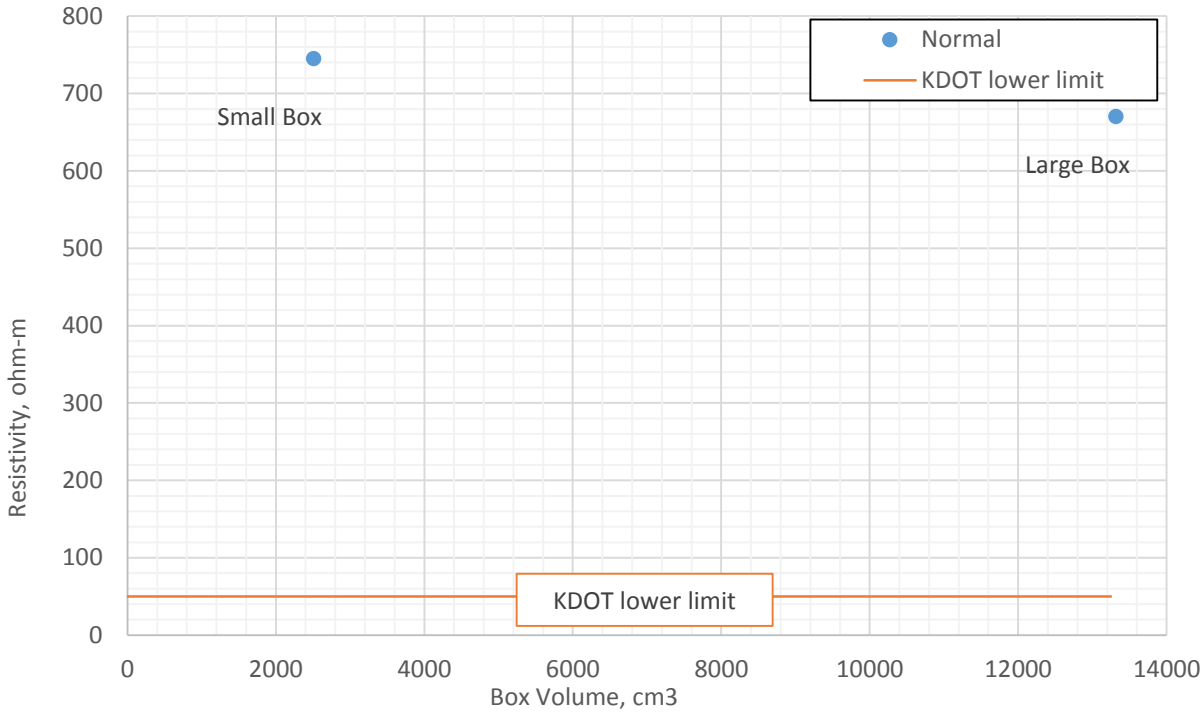

Figure A.15: New ASTM Colored I70/K7 Resistivity Results vs. Box Volume